Sigma Xi Student Research Poster Session

21-22 September 2017

Eldridge Commons, Swarthmore College

Sigma Xi The Scientific Research Society
Swarthmore College Chapter
"Companions in Zealous Research"

Poster locations for the 2017 Sigma Xi poster session

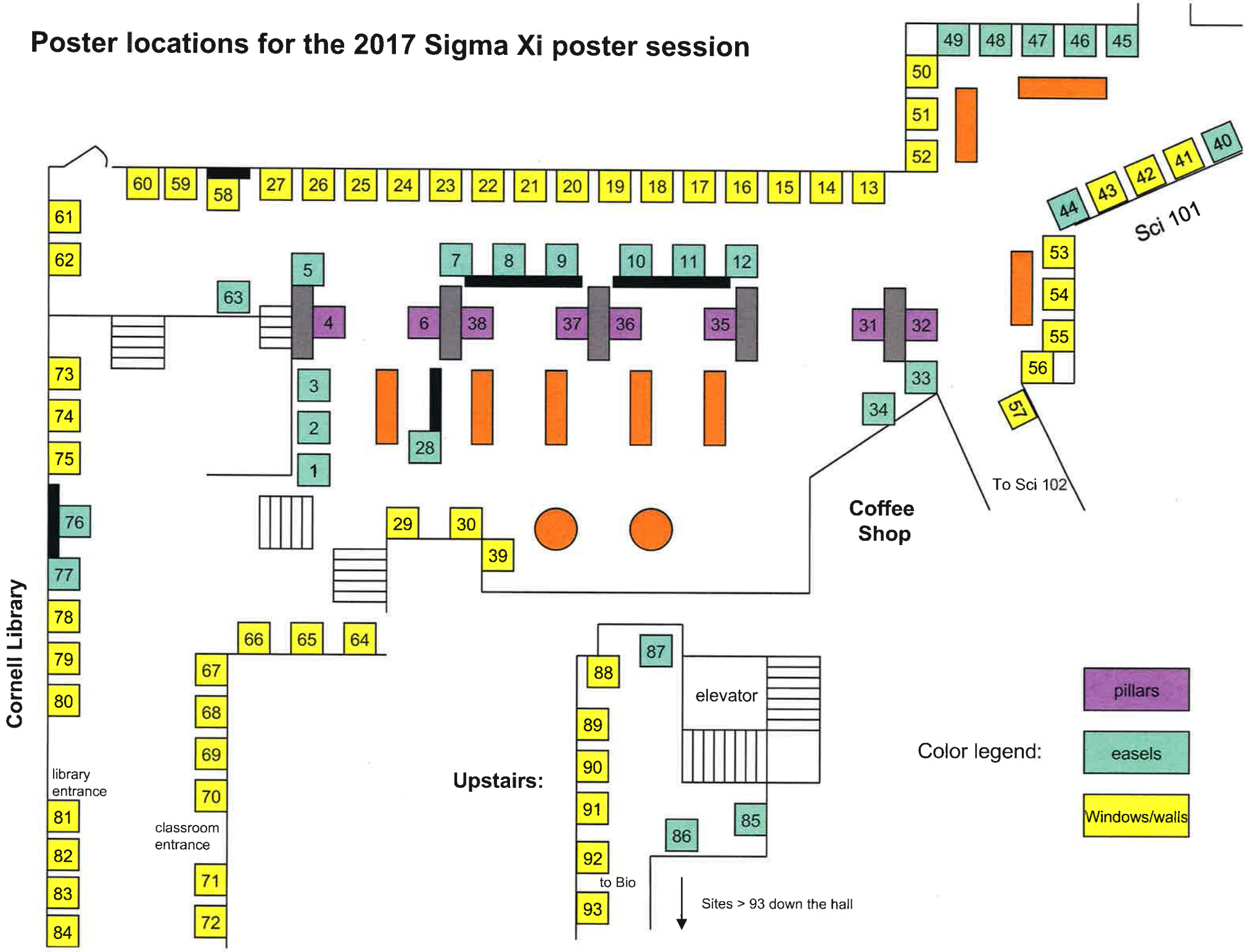

85	Abitino, Angelina	Measuring Catastrophic Forgetting in Neural Networks	Computer Science
62	Adhikari, Hriju	Effect of Plant Species Richness on Parasite Burden in Mice	Biology
11	Barbano, Luke	Characterizing the volume of a compressed Taylor state object in the SSX plasma	Physics
63	Barreto Corona, Guillermo	Co-occurrence based estimates of mammal-dung beetle interaction networks across a deforestation gradient	Biology
51	Barros Guinle, Maria Isabel	Set size cuing leads to faster recognition in a short-term memory task	Other
49	Bush St George, Calla	Correlation between parasite load, diet, and body condition index in Peromyscus leucopus and P. maniculatus	Biology
75	Charo, Ben	Infection and Proliferation Rates of Heat Resistant and Heat Sensitive Zooxanthellae in Aiptasia under Different Temperature Conditions	Biology
2	Chen, Tianlu and Devon Loehr	Demand-Driven, Higher-Order Static Analysis of Python Source Code	Computer Science
17	Chiang, Taylor	A Simple Stepwise Process for 3D Printing Bony Structures for Surgical Applications	Other
21	Clark, Alexa (Scout)	Measurement of Root Growth Rate in Arabidopsis	Computer Science
13	Deb, Moniher and Nicholas Ambiel	Using RT-MLPA Methods to Screen for Multiple Viral Pathogens in Honey Bees	Biology
23	Dellal, Daniel	The Effect of microbiota colonization on Neutrophil and Hematopoietic stem cell development in embryonic Zebrafish	Biology
20	Dong, May	Characterization of Mutant Universal Stress Protein A in Escherichia coli	Biology

69	Dow, Nathan	Functionalization and Characterization of Enantiopure Planar Chiral Î·4-Iron(0) Tricarbonyl Diene Complexes For Use in Stereoselective Transformations	Chemistry
47	Dreier	The mitotic kinase CDK1 inhibits FGF receptor degradation during heart founder cell division in the Ciona intestinalis embryo	Biology
37	Erler, Elizabeth	Mycobacteria models to further study the mechanism of small molecule inhibition of FadD32 in Mycobacterium tuberculosis.	Biochemistry
78	Figueroa, Mishel	Using Verteporfin to target the mechanotransduction downstream effector YAP/TAZ in FOP mutant mouse embryonic fibroblasts	Biology
58	Flores, Elizabeth	Dung beetle - fecal parasite interaction networks across a deforestation gradient	Biology
77	Fornof, Lillian	The Ecological Factors Influencing Behavior of Forked Fungus Beetles (Bolitotherus Cornutus)	Biology
8	Franklin, Maxwell	The Role of Self Efficacy (SE) in Introductory Physics	Physics
6	Gao, Allan	Structural Studies of Non-Canonical Secondary DNA Structures Interacting with Small Molecule Ligands	Chemistry
86	Garba, Saadiq	Social grouping Behavior in Small and Large Populations of Bolitotherus Cornutus	Biology
82	Green, Daniel	Characterizing an Unidentified Plasma Fluctuation Using Fourier Analysis of Imaging Data and Fitting Techniques	Physics
50	Gu, Jerry	Lorber Opentalk Project 2017	Engineering
54	Hejna, Ben	Diastereomerically Selective Intramolecular Rh(II) Catalyzed C-H Insertions of Enantiomerically Pure N-Oxazolidinoyl Iron(0) Tricarbonyl Dienes	Chemistry
30	Hernandez, Jesus	A Low Cost Agile Robot for Outdoor Collectives	Engineering

27	Himelein-Wachowiak, McKenzie	Cloning vomeronasal type-2 receptors to elucidate pheromonal signal transduction in Mus musculus	Biology
52	Holmes, Aaron and Ben Hsiung	Investigating amantadineâ€™s membrane partitioning behavior and induced conformation changes in the Influenza A M2 protein	Biochemistry
28	Ingersoll, Maria	Arbovirus surveillance through avian serum in Eastern Oklahoma and Eastern Texas	Biology
67	Jacobs, Brent	Differential Privacy: Selecting the best protocol	Computer Science
70	Jansen, Andrew	Development of a Bode Plot Generating Website	Engineering
24	Jordan, Deondre	Surveying the fold of DNA repeats associated with replication fork collapse	Biochemistry
36	Keezing, Umi	Differential Directional Bias in Azimuth and Elevation	Psychology
80	Kim, Elise	Functionalizing single-walled carbon nanotubes with photocleaving [Ru(phen)2(L-aap)]2+ as a potential mode of drug delivery	Biochemistry
48	Kim, Hyeongmin	Effectiveness of ultrasound and microbubbles in dissolving thrombi in vitro	Engineering
16	Kissman, Elijah	The Expression and Purification of Quorum Sensing transcriptional regulator LsrR from Escherichia coli	Biochemistry
42	Kwok, Katherine and Keton Kakkar	Transcription Factor Binding Site Prediction Using Neural Networks	Computer Science
40	Lamberty, Zach	Click Surface Modification for Controlled DNA Immobilization	Engineering
71	Lanphear, Elizabeth	Response of Zooxanthellate Aiptasia Pallida to Flow	Biology

43	Lee, Bo Lim (Linda) and Elise Kim	Functionalizing single-walled carbon nanotubes with [Ru(bpy)2dppz]2+ as a potential mode of drug delivery	Chemistry
60	Li, Jessica	Saving the Best for Last: IPLS as a Capstone	Science Education
44	Li, Sida	Robustness of balancedâ€"state model.	Mathematics
32	Lifset, Noah	SETI L-band Data Recovery and Analysis	Astronomy
53	Lin, Jennifer	Using Rhesus Monkeys to Model the Social Striatum	Biology
19	Lin, Yingqi (Linda)	Biophysical and structural studies of telomeric DNA in complex with a small molecule ligand as an anticancer strategy	Biochemistry
45	Llosa, Isabel	Evolution of the [i]Ciona intestinalis[/i] Heart Gene Regulatory Network	Biology
35	Malisa, Jessica and Emily Ferrari	Transfecting normal human cells to express Human Satellite 2	Biology
3	McLeish, Colin	Ultrasonic method and device for monitoring muscle water content	Engineering
18	Min, Do June	Will deception work in FlipIt security games?	Computer Science
74	Morriss, Julia	Selecting an aptamer to bind insulin-like growth factor 1	Biochemistry
68	Mosneanu, Rares	Heterobimetallic Aluminum-Alkali Metal Complexes of New Tetraanionic Chiral Ligands for Asymmetric Catalysis	Chemistry
57	Mundo, Jake	Zero-Diagonal Minimum Rank	Mathematics

38	Nasrallah, Sophie and Isabel Erickson	Characterization of hummingbird microbiomes in relation to fattening cycles	Biology
84	Ngo, Lan	Combining Independent Confidence Intervals to Account for Uncertain Ages in Paleontology	Statistics
64	Nogueira, Natasha	Utilizing statistical analysis to develop a python algorithm to constrain orbits of young binary systems	Astronomy
26	Nyovanie, Samantha	Toward structure of the G-quadruplexes formed by VEGF and G4TERT	Biochemistry
33	Ogolla, Timothy	Pitch and Helical Twisting Power Measurements in Chiral Chromonic Liquid Crystals	Physics
15	Parrish, Bennet	Investigating the soil mycorrhizal fungal community composition of invasive plant species in the Crum Woods	Biology
14	Petty, Nicholas	Examining the structural and functional properties of the Thermobacillus composti ortholog of autoinducer-2 receptor LsrB	Biochemistry
65	Portley, Makayla	Streptococcus pyogenes activates sensory neurons to release CGRP, inhibiting neutrophil killing	Biology
73	Potluri, Rajiv	Where's The Junk?: Mapping HSATII in the Human Genome	Biology
7	Powell, Barrett	Efforts towards the crystal structure of a noncanonical DNA repeat implicated in cancer	Chemistry
41	Purcell, Morgan and Christina Labows	Irrelevant speech suppresses verbal rehearsal	Other
9	Qaddura, Yusuf	Analysis of the Spread of Vector Borne Diseases with Delay Differential Equations	Mathematics
66	Rabin, Alexandra	Investigation of the therapeutic potential of combining CDK7, CDK12/13, and BET inhibitor strategies in Small Cell Lung Cancer	Biology

61	Rao, Arka and Laela Ezra	Characterization of Silver Nanoparticle Behavior via Electrochemical and Spectroscopy Analysis	Chemistry
55	Raymond, Hayley and Abigail Wong	Structural Studies of the Influenza A M2 Membrane Protein Critical to Viral Budding and Genome Packing	Biochemistry
56	Reische,Elijah	The role of the cytoskeleton in FGFR trafficking in Ciona intestinalis	Biology
83	Reyes, Jordan	Relative contributions of mammal and habitat on dung beetle community structures across a deforestation gradient	Biology
1	Robinson, David	CMB Constraints on Spatial Anisotropy of the Fine-Structure Constant	Physics
22	Shrock, Jaron	Acceleration and Compression of Taylor State Plasmas on SSX	Physics
81	Simon-Plumb, Casey Lu	Pediatric Second Primary Thyroid Cancer: Epidemiologic Characterization & Radiation Implication	Other
31	Sokota, Samuel	Using Neural Approximations to Solve Games	Computer Science
34	Spencer, Sierra	Biofuels at Swarthmore	Engineering
29	Stant, Elizabeth	Investigation of Sema6a Reverse Signaling and the Role of Secreted Sema6a	Other
10	Suen-Lewis, Emma	Precision Electron Density Measurements in the SSX MHD Wind Tunnel	Physics
39	Sung-Clarke, Serena	Innate Immune Interactions in Aiptasia pallida	Biology
72	Tan, Wendy	Propranolol as an adjunct to exposure therapy in the treatment of pathological fear memory: an animal model	Psychology

25	Tostado-Marquez, Jonathan	Failed Power Domination	Mathematics
88	Traore, Soumba	Investigating the effects of antioxidants SkQ1 on mtDNA in PolG mouse fibroblasts	Biology
46	Tumey, Cameron	Exploration of Asymmetrical Gene Expression within Ciona Intestinalis	Biology
87	Velleca, Anthony	Validating PTCHD1 removal from knockout mice lines that utilize Cre- lox recombinase system	Biology
5	Williams-Nicholas, Zara	Zero-Diagonal Minimum Rank over Generalized Fields	Mathematics
79	Wilson, Henry	Aluminum complexes of Redox Active Î±-diimine Ligands	Chemistry
12	Woodside, Audra and Mackinsey Smith	Aluminum Complexes of Nitroxide-Based Redox-Active Ligands	Chemistry
76	Yan, Fengjun	Learning Deviation Payoffs in Large Symmetric Games	Computer Science
4	Yeung, Brandon Chung Yuen	Simulating fibrin clot mechanics using finite element methods	Engineering
59	Youn, Gun Min	Microplastic pollution and its effects on Aiptasia pallida	Biology

Measuring Catastrophic Forgetting in Neural Networks

Angelina Abitino, Dr. Christopher Kanan

Rochester Institute of Technology
aabitin1@swarthmore.edu

Deep neural networks are used in many state-of-the-art systems for machine perception. Once a network is trained to do a specific task, e.g., bird classification, it cannot easily be trained to do new tasks, e.g., incrementally learning to recognize additional bird species or learning an entirely different task such as flower recognition. When new tasks are added, typical deep neural networks are prone to catastrophically forgetting previous tasks. Networks that are capable of assimilating new information incrementally, much like how humans form new memories over time, will be more efficient than re-training the model from scratch each time a new task needs to be learned. There have been multiple attempts to develop schemes that mitigate catastrophic forgetting, but these methods have not been directly compared, the tests used to evaluate them vary considerably, and these methods have only been evaluated on small-scale problems (e.g., MNIST). In this paper, we introduce new metrics and benchmarks for directly comparing five different mechanisms designed to mitigate catastrophic forgetting in neural networks: regularization, ensembling, rehearsal, dual-memory, and sparse-coding. Our experiments on real-world images and sounds show that the mechanism(s) that are critical for optimal performance vary based on the incremental training paradigm and type of data being used, but they all demonstrate that the catastrophic forgetting problem has yet to be solved.

Effect of Plant Species Richness on Parasite Burden in Mice

Hriju Adhikari, Courtney A. Thomason, Ph.D

Mountain Lake Biological Station, Pembroke, Virginia
hadhika1@swarthmore.edu

Among many interspecific relationships, parasitism is a relationship that involves an ongoing co-evolutionary arms race between host and parasite (Sadava *et al., 2011*). One way that hosts might defend themselves against harmful parasites is through their diet by self-medicating themselves (Lozano, 1998). One anti-parasitic property of plants that animals consume is tannin, plant polyphenols that can precipitate proteins (Horvath 1981), which have also been shown to reduce parasite loads and cure animals from their illnesses (Villalba and Provenza, 2007). We examined the correlation between plant species richness and parasite burden in mice to understand the extent to which plant diversity helps reduce parasite burden in the mouse population. We collected plant samples and mouse fecal samples from two different mouse trapping grids and analyzed the fecal samples via fecal floatation for parasites. We used generalized linear models to analyze the effect of plant species diversity on mouse parasite burden. This study ultimately suggests that higher oak availability may be tied to acorn consumption. As mice consume more acorns, which seem to have high tannin concentration, they will have lower parasite burden.

Characterizing the volume of a compressed Taylor state object in the SSX plasma

Luke Barbano, Michael Brown

Swarthmore College
lbarban1@swarthmore.edu

A cookbook of numerical techniques (namely wavelet transforms, smoothing filters, and spline interpolations) is applied to characterize the length (and thus the volume) of a stagnating Taylor state object in SSX. This length analysis uses magnetic field data from a linear array of 20 evenly spaced 2-D $\dot{B}$ probes along the compression can axis. A 3-D animation of the Taylor state object's magnetic field in the compression volume reveals the object's wavelet-like magnetic structure in space. In order to localize the object in space and characterize its length, a continuous wavelet transform using a Paul parent wavelet of order 2 is performed. The most dominant spatial frequency given by the resulting frequency-space spectrogram is taken to be the length of the object in the compression volume. This length, in conjunction with the cross-sectional area of the compression can, gives the object's volume. Information about the object's volume as a function of time allows us to identify instances of compressive heating and investigate the magnetothermodynamics (MTD) of the SSX plasma.

Co-occurrence based estimates of mammal-dung beetle interaction networks across a deforestation gradient

Guillermo Barreto Corona, Elizabeth Nichols

São Paulo, Brazil
gbarret1@gmail.com

Tropical deforestation is a global environmental change driver, with demonstrated impacts on biodiversity. However, how native forest loss influences key species interactions, including those between mammal fecal donors and dependent fecal detritivores, remains surprisingly poorly characterized to date. Abundance evidence suggests that primary extinction of mammals in a given site produced secondary co-extinctions of dung beetles. We selected twelve independent 3km landscapes in the Atlantic Forest of São Paulo, Brazil, where all landscapes were constrained to similar soil types, elevation ranges and slopes, but spanned a 10-60% forest cover gradient. We distributed eight sampling points within each landscape using a stratified, random proportional selection process based on largest fragment size. At each point, we simultaneously collected data on dung beetle and medium and large-bodied mammal community structures in 2015, using well-replicated and standardized methods (i.e. baited pitfall traps and camera traps). We finally used environmentally constrained co-occurrence modeling to estimate the structure of mammal-beetle interaction network structure at each sampling point – we used the c-score method. We captured 2,598 beetle individuals in 35 species across 11 genera, and registered 19 mammal species across the 12 focal landscapes. Preliminary analysis suggests that native forest cover loss was associated with reduced network connectance, primarily through reduced species richness of dung beetles (rather than through effects on mammals). Out of 11 landscapes and 2,770 possible mammal-dung beetle species pairs, we only detected 8 co-occurring species pairs. Out of these, 6 demonstrated aggregation and 2 segregation. Because of this we could not use generalized mixed models because of minimal co-occurrence results found. From our results we can assume that strong ecological filtering has potentially homogenized both mammal and beetle communities.

Set size cuing leads to faster recognition in a short-term memory task

Maria Isabel Barros Guinle, Lisa Payne

Swarthmore College
mbarros1@swarthmore.edu

Short-term memory (STM) is the temporary representation of information in our mind. The widely used Baddeley and Hitch (1974) multicomponent model of STM proposes distinct mechanisms for holding verbal information via an articulatory loop and for holding visually represented information via an iconic visuospatial sketchpad. For example, the Sternberg task (1966) that requires a sequential set of letters to be held in short-term memory, has been historically associated with verbal STM. On the other hand, a task that involves holding a spatial array of colored squares in short-term memory is associated with visual STM. It is not known how much these processes interact during STM for verbal information with a visual-spatial component. Previous research has shown that cueing the location of stimuli in a visuospatial task can improve memory recall. The current study aimed to examine the influence of visuospatial cuing on short-term memory for verbal stimuli. In this modified version of the Sternberg task, sets of 2, 4, or 6 consonants were presented simultaneously on a computer screen. For half of the participants, a spatial cue indicating the size of the upcoming memory set preceded the presentation of the letters. For all participants, following a brief retention interval, a probe letter appeared and they indicated whether or not the probe had been present in the memory set. The results revealed faster reaction times to the probe when participants were cued prior to each trial with which of the three set sizes to expect. When assessing the reaction times within each set size (2, 4, or 6), results showed the same trend across all three memory set sizes. Faster recognition when the set size is cued demonstrates that spatial cuing is effective in a verbal STM paradigm. Future work is needed to determine whether the effect of this spatial cue was due to an interaction between verbal and visual STM, or whether the cueing increased the likelihood that visuospatial STM would be successfully utilized despite the verbal nature of the stimuli.

Correlation between parasite load, diet, and body condition index in *Peromyscus leucopus* and *P. maniculatus*

Calla A. Bush St George, Courtney A. Thomason

Mountain Lake Biological Station University of Virginia
cbushst1@swarthmore.edu

Individuals in a species can have immune systems with varying responses to similar parasites, different parasite burdens. Two responses are resistance, fighting against and trying to rid the organism of the parasite, and tolerance, limiting the negative effects of the parasite without ridding the body of it (Raberg et al. 2009). Recent research by Justine Hamilton has shown that higher numbers of *Peromyscus leucopus* and *P. maniculatus* display tolerance rather than resistance to parasite infections (Hamilton 2017). My main hypothesis is that a high protein diet will correlate with a low body condition index (BCI). A low body condition in a mouse would signify low fat storage in a mouse when compared to other similarly sized mice. My secondary hypothesis is that diet resources correlate with resistance and tolerance mechanisms, a diet high in protein allows a mouse to have a stronger immune system, whereas when a mouse has a diet high in fat the mouse has a weakened immune system and immune responses (Hamilton 2017).
This research was performed at Mountain Lake Biological Station. *Peromyscus leucopus* and *P. maniculatus* were captured on two half hectare trapping grids with Sherman Live Traps and were weighed, body length recorded, and treated with either anthelmintic medication or a control sugar water solution. Fecal samples were collected from each mouse at each capture to monitor parasite infection burdens via fecal salt floatation and compound microscopy and for a future diet metabarcoding analysis. A script previously generated by Dr. Courtney Thomason in Program R to use a mouse's body measurements and weight to determine a score that shows an estimate of the mouse's body fat content. Body condition score was calculated with a scaled mass index defined by Pieg and Green (2009) and modified from the Thorpe-Leonart model of scaling. The body condition index, BCI, when compared with the parasite infection intensity of a mouse will give an approximation of how tolerant a mouse is to parasites. We used repeated measures analysis of variance (ANOVA) to determined whether insect species richness and presence of dominant insect species impacted mouse BCI, and whether infection intensity altered this relationship at all. There were no significant effects of the parasite load and the plant and insect species richness on BCI. There were also no significant effects of the most common species of insects, Carabidae, and plants, Blueberries and Oaks, on mouse BCI. Mouse sex and age were the only significant factors in determining parasite load.

Resources:
(1) Chandra RK. 1997. Nutrition and the immune system: an introduction. (2) Hamilton J. 2017. Diet and selection and parasite infection in peromyscus leucopus and p.maniculatus: do wild mice alter foraging behavior to combat intestinal parasites. (3) Raberg L., Graham A.L., and A.F. Read. 2009. Decomposing health: tolerance and resistance to parasites in animals.(4) Peig J., and A. J. Green. 2009. New perspectives for estimating body condition from mass/length data: the scaled mass index as an alternative method. Oikos. 118: 1883–1891.

Infection and Proliferation Rates of Heat Resistant and Heat Sensitive Zooxanthellae in *Aiptasia* under Different Temperature Conditions

Ben Charo, Rachel Merz

Swarthmore College
bcharo1@Swarthmore.edu

Corals contain endosymbiotic dinoflagellates known as *Symbiodinium*. These organisms photosynthetically produce a significant amount of organic material for their hosts in exchange for nutrients and protection. Under stressful scenarios, corals may expel their symbionts, causing the animal to whiten in a process known as bleaching. Though symbionts may be taken up from the surrounding environment if stress is ameliorated, bleached corals have a high risk of mortality. As oceans warm, this process has contributed to more frequently occurring global mass bleaching events and the precipitous decline of reefs worldwide. Some corals, however, may be more resilient than others. Indeed, certain clades and subtypes of *Symbiodinium* have been shown to confer heat resistance, yielding more robust symbioses. Relatively little is known, however, about whether these resilient *Symbiodinium* are more likely to infect and proliferate within a host under heat stress. The present study sought to address this issue by comparing infection and proliferation rates for two strains of Clade A *Symbiodinium*, one heat sensitive (SSA02) and one heat resistant (SSA03), in the model organism *Aiptasia*. Results showed SSA02 to infect and proliferate in *Aiptasia* more effectively under both conditions. However, SSA02 infectivity and proliferation rates declined substantially in hotter conditions while SSA03 infectivity and proliferation rates remained relatively constant. These data suggest that while SSA03 functionality might be maintained under heat stress, SSA02 is still preferentially taken up and reproduces more quickly. By extension, it's possible that heat sensitive symbionts may be taken up more often by corals even in adverse conditions. Given the contamination of controls and lack of certainty surrounding SSA03 infection, however, future studies are required to confirm these findings.

Demand-Driven, Higher-Order Static Analysis of Python Source Code

By Tianlu Chen and Devon Loehr, advised by Zachary Palmer
Swarthmore College
tchen2@swarthmore.edu, dloehr1@swarthmore.edu

The Python programming language is widely used today, by programming beginners and veterans alike. However, due to its structure certain classes of errors are very common -- for example, type errors. To combat this, we aimed to develop a tool which could be used to analyze Python code to determine certain aspects of its behavior at runtime. This work builds on previous work by first simplifying the Python code, then embedding it into an abstract pushdown system (PDS) and finally running a PDS reachability analysis which, given a snippet of code, a line number and a variable name, returns a set of possible values that the variable can be bound to at that line. We have successfully implemented a barebones analysis for a small subset of Python by now, and plan to expand the scope of the analysis in the near future.

A Simple Stepwise Process for 3D Printing Bony Structures for Surgical Applications

Taylor Chiang, Robert Pugliese

Jefferson University, Philadelphia, PA
Tchiang1@swarthmore.edu

Three-dimensional printing has existed for 30 years, however more recently this methodology has increasingly been used in a variety of biomedical applications, including implants, models, medical devices, and prosthetics. This report outlines the general workflow for 3D printing of any bony structure for preoperative surgical planning and preparation, with special application in free fibula flap (FFF) mandibular reconstructive surgeries. This paper is also a proof-of-concept study with two patients in our pilot. During FFF mandibular reconstructive surgeries, titanium plates must be inserted into a patient's mouth, however the time to bend these plates intra-operatively can take up to an hour. Our technique involves the use of the following open-source programs-- 3D Slicer, Meshmixer, and Cura-- to 3D print patient specific mandibles in order to pre-bend plates using these models as a guide. By converting DICOM files to STL files in 3D Slicer, it is possible to clear away soft tissue and isolate the needed anatomy in Meshmixer, convert to a 3D printable file in Cura, and input the file to an FDM 3D printer (using, in this case, an Ultimaker 2+ Extended). We provide a detailed description of each step required to print an accurate, patient-specific mandible replica from the CT scan. The results from our two patient pilot showed sufficient accuracy of patient specific 3D printed mandibles considering minor or no adjustments were made to the pre-bent plates used for mandibular reconstructive surgery. Our results also suggest the use of pre-bent plates may decrease operating time. The application of digital manufacturing of patient specific bone models using consumer grade desktop 3D printers can be demonstrated through the use of custom mandibular anatomical models in mandibular reconstruction surgery. The models represent the potential benefits for procedural planning, surgical training, operating room efficiency, and patient education. The design of this workflow can be applied to a variety of anatomical interests, specialties, and surgical applications, and is not limited to bony structures or otolaryngology procedures.

Measurement of Root Growth Rate in Arabidopsis

Scout Clark, Nick Kaplinsky, Ameet Soni

Swarthmore College
aclark2@swarthmore.edu

Analysis of plant response to heat shock has implications for agriculture and human health, specifically with regard to cellular mechanisms that are similar to those in Alzheimer's, Parkinson's Disease, and cancer. As such, root growth rate measurement provides insight into how plant cells sense and respond to high temperatures. Datasets consisted of 180 images of each plant root over a 12 hour heat shock time period. The images exhibited variable exposure due to differences in Green Fluorescent Protein (GFP) expression and due to mutable growth patterns. Computer vision and image processing techniques were used to transform the inconsistent images into simpler datasets to allow for efficient, accurate, and automated root growth rate measurement.

The compilation of root lengths for each image generated the overall root growth rate datasets. Lengths were determined through the use of a medial axis transform, which "skeletonized" the root object to form a traceable template to obtain root distance.

A Graphical User Interface (GUI) was developed as a user-friendly interface for researchers who will use this software. Root growth rate data can be transformed into *Length vs. Time* and *Displacement vs. Time* graphs, as well as into time-lapse videos.

The *Root Tracker* interface reliably generates root growth rate measurements for mutants of Arabidopsis and improves the efficiency of the data processing. Future studies will consist of the automation of the RootScope (i.e. the microscope used for imaging) to track full heat response. Additionally, the image processing software can be edited to automatically find each preliminary root position.

Updated Abstract Draft: Moniher Deb '19 and Nick Ambiel '19
Title: Using RT-MLPA Methods to Screen for Multiple Viral Pathogens in Honey Bees

The western honeybee (*Apis mellifera*) is a crucial pollinator that maintains our national food security and general biodiversity. The multifactorial stressors that pertain to the population decline includes pesticide exposure, poor nutrition, parasites, and loss of foraging habitat. Being such a pivotal aspect of our wellbeing, a more holistic approach is needed to characterize the factors responsible for the global decline in honeybee health. As part of a larger collaborative effort, that seeks to explore correlations between the bee hive exposome and indicators of bee health such as parasite loads, we characterized the relative abundance of multiple viruses at once using a Reverse Transcriptase Multiplex Ligation-dependent Probe Amplification (RT-MLPA) assay, over a 3 month period, from 30 hives at 10 different local sites in Southeastern Pennsylvania. We found that bees sampled in August significantly have lower viral loads than bees sampled in September and there tends to be higher viral loads in more urbanized regions. Our analyses also indicate a number of positive and negative associations between different viral strains. Honey bees therefore do not necessarily head into winter with higher parasite burdens as previously suggested and beekeeping in urban areas may result in having less healthy bees. Lastly, the positive and negative associations between different viral strains in a single host supports the notion that they are likely to interact directly or indirectly with one another and impact the overall parasite burden found within the bee.

The Effect of microbiota colonization on Neutrophil and Hematopoietic stem cell development in embryonic Zebrafish

Daniel Dellal, Dr. Eva Fast, Dr. Leonard Zon

Harvard University
Ddellal1@swarthmore.edu

Neutrophils are cells which form part of the inflammatory response to infection and injury. (Kanther et al). Hematopoietic stem cells can differentiate into all blood cell types, and thus HSC transplants form an important role in immune response for individuals with compromised immune system cells, such as patients with multiple myeloma and leukemia (Birbrair, Frenette). While interactions between the environmental microbiota during embryo development and development of Neutrophils as well as HSCs is not yet fully understood, it has been shown that gnotobiotic zebrafish, did in fact show a decrease in neutrophil number (Kanther et al.). However, interactions between microbiota and HSC development have not yet been measured. In this experiment we attempted to understand this interaction by raising gnotobiotic embryos as well as control embryos and then observing the differences in HSC development using both *in vivo* imaging to measure cell number, as well as qPCR techniques to measure gene expression. We also attempted to replicate experiments in which neutrophil number was shown to decrease due to the absence of microbiota (Kanther et al.) once again using *in vivo* imaging as well as qPCR techniques to measure gene expression. We found that gnotobiotic embryos exhibited a lower number of neutrophils through imaging as well as gene expression through qPCR than control embryos, as was seen in previous experiments. We also found that HSC gene expression was found to be lower in gnotobiotic embryos than control embryos, however, imaging of HSC embryos was found to be inconclusive due to the dimness of the fluorescence. In future experiments, different HSC fluorescent lines of fish could be used to improve imaging, as well as more replicates of conditions in order to gain a more accurate assessment through qPCR. Different antibiotics and bacterial assessments could also be used to pinpoint exactly which species of microorganisms are causing the change in development between gnotobiotic and control condition embryos.

Characterization of Mutant Universal Stress Protein A in *Escherichia coli*

May Dong and Amy Vollmer

Swarthmore College

mdong1@swarthmore.edu

Universal stress protein A (UspA) is expressed across bacterial species in response to a wide variety of stressors, including nutrient starvation, antibiotic exposure, and oxidants. UspA is involved in maintaining stasis and has been shown to become phosphorylated at serines and/or threonines, but the mechanism and specific sites of phosphorylation are unknown. The Vollmer lab has systematically replaced each ser/thr residue with either alanine or aspartic acid to either prevent phosphorylation or mimic constitutive phosphorylation, respectively. We expect that some mutants should have abnormal growth or stress response when compared to wild type if the mutant locus is phosphorylated in response to stress.

Functionalization and Characterization of Enantiopure Planar Chiral η^4-Iron(0) Tricarbonyl Diene Complexes For Use in Stereoselective Transformations

Nate Dow, Dr. Robert S. Paley

Swarthmore College, Swarthmore, PA 19081
ndow1@swarthmore.edu

Multiple projects were investigated over the course of the summer to further the Paley lab's contributions to methodologies in asymmetric synthesis, primarily concerning planar chiral $Fe(CO)_3$ – diene complexes and their potential uses in stereoselective reactions. First, investigation of the stereochemistry of $Fe(CO)_3$ moieties complexed to dienes diastereoselectively using N-oxazolidinonoyl chiral auxiliaries was conducted via X-ray crystallography and Circular Dichroism (CD) spectroscopy. The crystal structure obtained this summer confirmed the absolute stereochemistry predicted by the lab's previous work and suggested a pattern for the formation of major diastereomers during complexation. A second project resulted in the novel synthesis of the most structurally demanding N-oxazolidinoyl complex formed yet by the Paley group. Based on the product's unique indole-functionalized structure, it is expected that this compound could be used as a substrate for a novel diastereoselective Pictet-Spengler sequence, mediated by the planar chiral $Fe(CO)_3$ unit to selectively form new stereocenters. Other investigations included the attempted syntheses of new chiral auxiliaries, such as cyclic ureas and sulfonamides, to improve the diastereoselectivites observed for complexation reactions.

The mitotic kinase CDK1 inhibits FGF receptor degradation during heart founder cell division in the *Ciona intestinalis* embryo

Matthew Dreier, Christina D. Cota, and Brad Davidson
Swarthmore College
mdreier1@swarthmore.edu

During cell division, cell components must be properly segregated and inherited. The proper segregation of cell surface receptors is particularly important because abnormal signaling can lead to developmental defects or cancer. Membrane trafficking can contribute to receptor segregation, but little is known about membrane trafficking during mitosis or the mechanisms that control it. Here we show that the mitotic regulator cyclin-dependent kinase 1 (CDK1) influences membrane trafficking by shielding FGF receptors from lysosomal degradation during cell division. CDK1 inhibited degradation in both fixed and *in vivo* studies and at multiple stages of mitosis. Our results suggest a previously unknown role for the regulators of mitosis in coordinating mitotic membrane trafficking. By uncovering mechanisms that control mitotic membrane trafficking, these data define new pathways that regulate cell signaling. An understanding of these pathways may suggest how improper segregation can lead to abnormal cell fate, behavior, or malignancy.

Mycobacteria models to further study the mechanism of small molecule inhibition of FadD32 in *Mycobacterium tuberculosis*.

Elizabeth Erler, James Gomez and Samantha Wellington

Broad Institute, Cambridge, MA
eerler1@swarthmore.edu

Infection with *Mycobacterium tuberculosis* (Mtb) remains a global health threat and accounted for 1.8 million deaths in 2015, surpassing HIV/AIDS as the single most deadly infectious disease[1]. The rise of multi-drug resistant TB (480,000 cases in 2015) adds urgency to the search for new drugs that will be effective in patients with resistance to one or more drugs[1]. The Hung lab identified a small molecule which is effective at killing Mtb cells and targets the enzyme FadD32. FadD32 is critical in the last steps of mycolic acid biosynthesis, a pathway targeted by frontline drug isoniazid and several other anti-TB drugs. In vitro biochemical assays suggest that the compounds work in two ways; first, by inhibiting the second enzymatic step, the transfer of a mycolic acid substrate to protein pks13, and second, by inhibiting an intermediate step in which the mycolic acid substrate is covalently bonded to the FadD32 enzyme. We hypothesized that this intermediate self-loading step could occur at one of three conserved cysteines in FadD32 through palmitoylation. Models for Mtb research are necessary for increased safety and efficiency as Mtb must be contained in a BSL3 laboratory and has a doubling time of 15 hours. *Mycobacterium smegmatis* (Msm) is not sensitive to FadD32 inhibitors and we were unsuccessful in our efforts to create a sensitive strain using the O.R.B.I.T. strategy. Future efforts will attempt to correct the possible disruption of the operon, although this model may ultimately be impossible to build because of the FadD32 protein differences between the two species (Msm and Mtb). We showed that *Mycobacterium marinum* (Mma) is sensitive to the FadD32 quinoline inhibitors and attempted to use plasmids with a Mtb allele resistant to the inhibitors and a mutation at one cysteine to test the functional importance of each cysteine for FadD32 enzyme function, but were unable to establish resistance to the FadD32 inhibitors in Mma. Currently, there are ongoing efforts to troubleshoot both of these models and to test the importance of the cysteines using the same plasmids in Mtb.

[1] "Global Tuberculosis Report 2016." World Health Organization. 2016.

Using Verteporfin to target the mechanotransduction downstream effector YAP/TAZ in FOP mutant primary mouse embryonic fibroblasts

Mishel Figueroa, Alexandra Stanley, Eileen Shore, PhD

Shore Laboratory
McKay Orthopaedic Research Laboratory
Perelman School of Medicine at the University of Pennsylvania

mfiguer1@swarthmore.edu

Fibrodysplasia ossificans progressiva (FOP) is a genetic disorder resulting in heterotopic ossification in connective tissue such as skeletal muscle. In classical FOP, a mutated *ACVR1* gene leads to a single R206H amino acid substitution. This substitution results in an overactive ACVR1 receptor, a bone morphogenic protein (BMP) type I receptor. Ultimately, progenitor cells are incorrectly directed to undergo chondrogenic and osteogenic fate decisions.

Microenvironment stiffness (extracellular matrix stiffness) has the capacity to direct cells to undergo differential fate decisions; different stiffnesses can direct cells down different lineages. Cells interpret their microenvironment via mechanotransduction pathways, through which mechanical and physical forces are converted into biochemical signals. YAP/TAZ is a key downstream effector of mechanotransduction signaling and its localization (nuclear vs. cytoplasmic) is associated with differential cell fate decisions and morphology; specifically, increased nuclear YAP/TAZ is associated with osteogenic fate decisions and morphology. The nuclear localization of YAP/TAZ has been shown to be elevated in FOP mutant cells as compared to wild type cells. As a result, we consider the possibility that FOP mutant cells may be misinterpreting their microenvironment, which in turn may be contributing to their aberrant cell fates.

If FOP mutant cells are misinterpreting their microenvironment, molecules involved in mechanotransduction pathways may serve as potential therapeutic targets. Here, we assess the ability of the small Verteporfin, which has been shown to inhibit YAP function, to mitigate the elevated nuclear localization of YAP/TAZ and rescue cell morphology in FOP mutant primary mouse embryonic fibroblasts. Using substrate stiffness assays, we find that the addition of Verteporfin significantly decreases nuclear YAP/TAZ localization at stiffness of 10kPa and 15 kPa but does not affect cell morphology.

Dung beetle – fecal parasite interaction networks across a deforestation gradient

Elizabeth M. Flores, Elizabeth Nichols

University of Sao Paulo, Sao Paulo, Brazil
eflores1@swarthmore.edu
enichol1@swarthmore.edu

For my project, we characterized patterns of interactions between dung beetles and the fecal helminth parasites they are intermediate hosts to across a deforestation gradient in the threatened Brazilian Atlantic Forest.

We measured network complexity using two metrics: connectance and interaction evenness. Connecatance is a qualitative metric that considers the proportion of realized links by total possible links. Interaction evenness is a quantitative metric that calculates the heterogeneity of links in a network. Interaction evenness was weighted by prevalence and infection intensity.

A total of 23 host-parasite networks from in 8 focal landscapes with different percentages of forest cover were described and modeled as a function of forest cover. We found that with more deforestation: (1) connectance was not related to forest cover when accounting for network size, (2) host-parasite interaction strengths were homogenized and (2) there were lower levels of infection.

These findings have implications in deepening our current understanding of the impact of deforestation on native habitat loss and interspecific interactions and, as a result, the the conservation tactics that would be most successful in protecting this ecosystem.

Ecological Factors Influencing Behavior of Forked Fungus Beetles (*Bolitotherus cornutus*)

Lillian Fornof, Vincent Formica

Mountain Lake Biological Station
lfornof1@swarthmore.edu

Forked Fungus Beetles, *Bolitotherus cornutus*, can be found on rotting logs, using various species of fungus as a resource for food and reproduction. The fungi also serve as social arenas where social networks are formed. In this study, thirteen wild populations were surveyed three times a day, during the morning, afternoon, and night, and behavioral and locational data were recorded of the beetles observed. Characteristics of fungal brackets and their location on populations were determined following the end of the season. Both datasets were combined to examine two types of measurements- ecological factors (age, size, species, and distance to closest bracket) and behavioral counts (use of bracket, number of observations, social interactions, and mating events). Of all ecological factors, distance to closest bracket was the only variable with no influence on behavior counts. Larger and younger brackets were more likely to be used and had more beetles on them while smaller and younger brackets had more social and mating behaviors. Although *Fomes fomentarius* brackets were more likely to be used, *Ganaderma applanatum* brackets had more observations and social and mating behaviors. Therefore, the most popular social arenas differed from the most used brackets, meaning that ecological factors have an effect on which brackets these social arenas are found and where the social networks of the population form.

The Role of Self Efficacy in Introductory Physics

Max Franklin, working with Dr. Catherine Crouch and Dr. Ben Geller
Swarthmore College
mfrankl2@swarthmore.edu

My research focuses on the change in different demographics in self-efficacy, concept tests, and attitudes over two semesters of physics. The first semester is a regular, pedagogically reformed mechanics course that contains both engineering and life science students. The second semester is split into two courses, a regular E&M course for engineering students and a reformed IPLS course for life science students. Students experienced different results based on both gender and major. Our biggest findings were in the realm of self-efficacy, where all groups came in with the same average self-efficacy. Over the first, mixed semester, the self-efficacy of women increased ($p=.11$), while the self-efficacy of other groups stayed the same. Then, over winter break, the SE of the women from both majors decreased, while SE of men stayed higher. The only group that experienced a significant gain in the second semester was that of women in biology ($p<.05$), who came in with the lowest SE but ended with the highest. Overall, men stayed at a high SE the entire year, while the women ebbed and flowed, with engineers showing high gains in the first semester and then regressing, while, biologists stayed the same at first then increased in the second semester.

There were also more slight changes in the concept tests and CLASS attitudes. In the first semester, men came in with significantly higher ($p<.05$) FMCE scores, but the women experience significantly higher gains such that the ending scores were the same. There were no differences by major. In the second semester, the students took the BEMA and there were no changes between genders and majors. For the CLASS in the first semester, women in engineering came in with much higher CLASS favorability scores than other groups, but no groups experienced significant changes overall. In the second semester among engineers, CLASS favorability scores for women decreased significantly, while favorability scores for men did not change.

Structural studies of non-canonical DNA structures implicated in anticancer strategies

Allan Gao, Liliya Yatsunyk

Department of Chemistry and Biochemistry, Swarthmore College
agao2@swarthmore.edu

G-quadruplexes, non-canonical structures of DNA, block gene transcription when they form. Thus, as they form predominantly in human oncogenes and telomeric DNA, g-quadruplexes have been increasingly studied in the past 20 years as anticancer agents. Here, we investigate the specific structural conformation of G-quadruplexes found in the oncogene promoter sequences c-Myc and Ac-Kit1. We used x-ray crystallography and biophysical analysis to study both DNA and DNA-ligand complexes. We producedcrystals for c-Myc and three different porphyrin bound derivatives: the copper derivative of 5,10,15,20-tetra(*N*-methyl-4-pyridyl)porphyrin (CuTMPyP4), ZnTMPyP4, and NMM. The native DNA crystals formed were large, uniform prisms, and the derivative crystals were rectangular prismatic, needle shaped, and square prismatic respectively. Furthermore, we were able to co-crystallize c-Myc with heavy atoms including sodium bromide, sodium iodide, hexamine cobalt (III), and cobalt (II) chloride. Native c-Myc crystals diffracted to 8Å. Preliminary biophysical studies and crystallization efforts on Ac-Kit1 will also be presented.

Social Grouping Behavior in *Bolitotherus Cornutus*

Saadiq Garba, Vincent A. Formica

Mountain Lake Biological Research Station
sgarba1@swarthmore.edu

Aggregation is a commonplace behavior in the animal kingdom. Many animals aggregate to feed, predate, defend against predation or to raise their young amongst other things. Some sexually dimorphic animals even sexually segregate during the non-mating season in preparation for the mating season. It is not uncommon to see large aggregations during the mating seasons of many animals. Formica et al found that more socially connected beetles (*B. Cornutus)*, have been shown to have higher reproductive success. However, social groups with more males has been shown to lead to less reproductive success. We speculate that this is due to male-male competition. Males spend more time fighting than courting females and thus drive down their reproductive success. To increase their reproductive success in social groups, larger males might surround themselves with smaller males who they can fight off. We, thus suspected that size and sex play a role in determining a beetle's social group. We found that not only do size and sex play a role in determining the size of a beetle's social group but also whether the beetle is from a large or small population. Sex and size were found to influence the number of social partners an individual had. However, the small and large populations did not have the same patterns. Population size also influenced how beetles socially grouped. Future studies could look at whether population size also affects others aspects of a beetle's social network and fitness.

Characterizing an Unidentified Plasma Fluctuation Using Fourier Analysis of Imaging Data and Fitting Techniques

Daniel Green, Adam Light

Swarthmore College
dgreen1@swarthmore.edu

The Controlled Shear Decorrelation Experiment – Upgrade (CSDX-U) is a cylindrical chamber in which argon gas is partially ionized into the plasma state. The plasma was confined and forced to rotate about the chamber's central axis by an axial magnetic field. A high-speed (50,000 fps) camera situated at one end of the chamber captured 10,000 frame videos of visible light emitted by the argon ions with a wavelength of 488 nm (ArII). Fourier analysis of the video files in both spatial (azimuthal) and temporal dimensions was used to generate dispersion plots of frequency vs wavenumber which revealed an unidentified fluctuation. Fitting techniques were then applied to characterize this fluctuation and estimate its propagation velocity through the plasma.

Lorber Opentalk Project 2017

Jerry Gu, Jasmine Charles, Kira Emmons, Pierce Forte, E. Carr Everbach

Swarthmore College
jgu1@swarthmore.edu

The purpose of this project was to improve upon a hands-free, voice-activated telephone device which allows a client to contact specific people without the use of the internet or concern of unwanted contact from strangers. After researching the capabilities of several hotword detection programs, the Raspberry Pi-based engine "Snowboy" was selected due to its reliability, accuracy, and security, among other features. The Snowboy engine was trained to detect the client's voice and place or end a call upon hearing specific keywords. A hardware component was then constructed which relies upon a voltage comparator, a 555 timer, and a mechanical relay to detect a rising edge in the circuit in order to hang up the phone when a call was finished. The system was later implemented into the client's household with limited success.

Diastereomerically Selective Intramolecular Rh(II) Catalyzed C-H Insertions of Enantiomerically Pure N-Oxazolidinoyl Iron(0) Tricarbonyl Dienes

Ben Hejna, Prof. Robert S. Paley

Department of Chemistry & Biochemistry, Swarthmore College
bhejna1@swarthmore.edu

For decades, the Paley lab has researched asymmetric organic synthesis through use of directing groups. Recently, the focus has turned to using a chiral oxazolidinone auxiliary to direct the addition of an iron(0) tricarbonyl unit to one face or the other of a diene. Facial selectivity of this reaction has been observed up to a 22:1 ratio of major:minor diastereomers. The newly added iron(0) tricarbonyl unit then allows for further diastereomeric direction on the periphery of the diene.

One of Prof. Paley's previous students successfully a 5-membered ring on the periphery of an iron(0) tricarbonyl diene by means of Rh(II) catalyzed C-H insertion. This created two new stereocenters, both of which were created with perfect (100:0) diastereoselectivity – however, it remains uncertain which diastereomer was formed.

Two more examples of perfectly diastereomerically selective C-H insertions were demonstrated through direction by the $Fe(CO)_3$ fragment. Both examples were similar in nature, differing from the original example by a longer tail and, in case of the second example, a different functional group on the tail. This demonstrates the viability of this reaction and its selectivity in a variety of environments.

Additionally, it was shown that the diazo functional group can be transferred to a methylene directly between a ketone and an $Fe(CO)_3$ diene by reaction with p-ABSA.

Future chemistry along this route will include projects such as the creation of more 100:0 diastereomerically selective C-H insertions, chemistry post-insertion, and attempting C-H insertions on diazo groups between ketones and $Fe(CO)_3$ dienes.

A Low Cost Agile Robot for Outdoor Collectives

Jesus Hernandez, Radhika Nagpal

Harvard University
jhernan3@swarthmore.edu

Currently, most terrestrial swarming robots are only functional within the lab. However, nature's self-organizing systems are not constrained to a lab environment. Our goal is to create a swarm of agile outdoor robots that can navigate autonomously using information from their surroundings and from each other in order to avoid obstacles and locate a target. The computer vision algorithms we implemented work well in a wide range of lighting environments, resulting in a swarm that operates robustly both indoors and out.

Cloning vomeronasal type-2 receptors to elucidate pheromonal signal transduction in *Mus musculus*

McKenzie Himelein-Wachowiak, Dr. Angel Kaur

University of North Carolina at Asheville
mhimele1@swarthmore.edu

This project contributed to efforts to create a library of ligand-receptor interactions in the house mouse (*Mus musculus*) vomeronasal organ (VNO), a sensory organ adapted for chemical signaling and pheromone detection. The specific aim of our project was to amplify reference vomeronasal type-2 receptor (V2R) sequences, which code for G-protein coupled receptors (GCPRs) in the VNO and clone them using first a bacterial *(E. coli)* plasmid. Following cloning, we intended to subclone the sequence in question into a mammalian expression vector so we could express the desired receptor in the Neuro 2A cell line. With expression limited to one V2R per cell, we could later pair individual receptors with specific mouse urinary proteins (MUPs) that serve as ligands in this context. Identifying these interactions hinged on the use of whole-cell recording to measure the changes in voltage that occur when a ligand successfully binds to and activates a receptor. Using the processes of polymerase chain reaction (PCR), gel extraction, and TOPO cloning, we successfully transformed several sequences coding for V2Rs into bacterial vectors. Additionally, we digested the plasmids in question using specific restriction enzymes in order to extract the sequence of interest so that we could begin moving it into a mammalian expression vector. Successful cloning and digestion was approximately verified using gel electrophoresis, and formally verified via Sanger sequencing. While it took several weeks to obtain proof of a full-length sequence transformation, we have reason to believe that the next step of transfection into Neuro 2A cells for the purpose of ligand pairing is not far off.

Investigating amantadine's membrane partitioning behavior and induced conformation changes in the Influenza A M2 protein

Aaron Holmes, Ben Hsiung, and Kathleen Howard

Abstract

The proton channel in the influenza A M2 protein is the target of amantadine and rimantadine, drugs that are no longer used in flu treatments due to increased antiviral resistance. Understanding how these drugs interact with M2 can facilitate the optimization of drugs targeting M2's proton channel. In this study, we introduce a novel NMR method to determine the membrane partitioning of amantadine and investigate drug-induced conformational changes of the full-length M2 protein using spin-labeling EPR spectroscopy. CW-EPR spectra show that a 1:1 drug:channel molar ratio is sufficient to broaden lineshapes of a residue in the M2 transmembrane (TM) domain. The change in the response to amantadine resembles the conformational change induced in spin labeled residues in response to cholesterol. To correlate these spectral changes to binding affinity, we sought to determine amantadine's partition coefficient in proteoliposomes. We developed an NMR protocol where we lyophilized the supernatant of M2 proteoliposomes with amantadine and ran the samples once they were rehydrated with D_2O. However, impurities were present in the spectra and could not be appropriately removed. Further studies into amantadine's partitioning behavior and the conformational changes through EPR can allow amantadine-M2 interactions to be better understood.

Arbovirus surveillance through avian serum in Eastern Oklahoma and Eastern Texas

Maria Ingersoll; Advisor: Matthew J. Miller
Sam Noble Oklahoma Museum of Natural History; University of Oklahoma; University of Texas Medical Branch
mingers1@swarthmore.edu

Birds are the most common hosts for arthropod-borne viruses (arboviruses) and play an integral role in disease dispersal across landscapes, as many species migrate hundreds of miles in a relatively short time span. Eastern Oklahoma and Texas fall along the Central Flyway, one of the migratory paths for many species that spend their winters in the neotropics. This is an important route for not only the avian fauna that make the journey but also for the viruses they carry. Many arboviruses such as West Nile Virus are known to circulate commonly in tropical climates such as Central America, yet their presence is also known in much of the southern United States. It is important to track any trends of these viruses as they circulate along the Central Flyway in order to make more astute observations about the risks they pose to human populations.

A few key viruses that take birds as their preferred host species and that have made a presence in the southern United States are West Nile Virus (WNV), Saint Louis Encephalitis Virus (SLEV), Eastern Equine Encephalitis Virus (EEEV), and Western Equine Encephalitis Virus (WEEV). The best way to track the circulation of these viruses in a particular location is to follow their movement through their hosts across a landscape gradient. Our team of researchers, led by Matthew J. Miller (Assistant Professor of Biology at the University of Oklahoma and Curator of Ornithology at the Sam Noble Oklahoma Museum of Natural History), spent the summer surveying Eastern Oklahoma and Eastern Texas for the prevalence of the four viruses mentioned above through sampling of over 30 species of wild birds (211 samples in total). Serum collected in the lab was processed at the University of Texas Medical Branch under the direction of Dr. Scott Weaver. There proved to be a significantly greater presence of total viruses from birds sampled in the southern-most site as compared to the other two locations, pointing to a conclusion that circulation of viruses along the Central Flyway becomes more prevalent closer to the equator, though it is spreading north. It also suggests that birds that act as hosts for these viruses are carrying viruses to the States, but that they are being transmitted to resident, non-migratory birds as well, as many of the birds that tested positive for antibody presence were residents.

Differential Privacy: Selecting the best protocol

Brent Jacobs, Dr. Lila Fontes

Swarthmore College
bjacobs1@swarthmore.edu

Anonymization, the removal from data of immediately identifying fields such as names or phone numbers, is often insufficient for ensuring privacy. Further, many privacy-protection methods lack a mathematical measure of the privacy protection being provided. Differential Privacy, pioneered by Cynthia Dwork and Aaron Roth, is a definition of privacy that quantifies upper bounds on privacy loss. Privacy-preserving protocols can be designed to meet the requirements of differential privacy; however, there is no standard way to judge protocols' utility. A novel way to compare protocols is to experimentally estimate the root mean squared error of the response distributions. While RMSE allows for comparing protocols, the relationships among them may not be straightforward to characterize.

Development of a Bode Plot Generating Website

Andrew Jansen, Erik Cheever

Department of Engineering, Swarthmore College
ajansen1@swarthmore.edu

Bode plots are frequently used in electrical engineering and control theory. These plots can be created approximately by hand or exactly using a program such as MATLAB®. The purpose of this program is to provide more accessible and interactive software for creating Bode plots using HTML and JavaScript. The program is intended to be a teaching tool to help students understand Bode Plots. Users can input a transfer function and the program and calculates the poles and zeros of the transfer function and creates the corresponding Bode plots. The program can also take inputted poles and zeros and output the appropriate transfer function and Bode plots. Important pole and zero cases such as repeated roots and complex conjugates are highlighted in the output. The interactive nature of this program allows students to see how changes in the transfer function or the pole and zero locations impact the Bode plot more clearly than with other software options.

Surveying the fold of DNA repeats associated with replication fork collapse

Deondre Jordan, Liliya A. Yatsunyk

Swarthmore College, Swarthmore, PA
djordan1@swarthmore.edu

DNA replication is a process essential to every living organism. Replication stress can lead to double strand breaks and replication fork collapse, ultimately promoting cancer. The CAGAGG DNA repeat has been identified in a bioinformatics study of the mouse genome as heavily associated with DNA breaks. We hypothesize that CAGAGG repeats form a stable secondary structure, capable of blocking DNA replication enzymes. Based on a variety of biophysical data (including circular dichroism (CD), UV-vis spectroscopy, and PAGE gel electrophoresis) we propose that CAGAGG repeat forms a tetrastranded, antiparallel structure with two GCGC tetrads stacked on top of each other and connected by GAGA loops. In order to test this model and gain further structural details, we have designed two sets of mutants. The first set is a series of 24 N-to-T single point mutants of the sequence 5'-AGG$(CAGAGG)_3$CAG-3' (also termed CA5-7), while the second set contains one, two, or three GCGC tetrads. The folding and thermal stability of mutants were analyzed via CD and UV-vis spectroscopies. Mutating any nucleotide in the GCGC core is detrimental to the stability of the structure leading to destabilization of ~ 15 °C; mutating GAGA loops changes the stability of the structure mildly, by no more than 5 °C. As expected, removing one GCGC tetrad decreases the stability of the structure, while adding one GCGC tetrad increases the stability. One tetrad introduces ~20 °C of stability to the CAGAGG structure. Our mutagenesis study strongly supports the proposed model. The presented data have great utility for understanding the structure of intrinsically difficult-to-replicate repeat sequences such as $(CAGAGG)_n$, and their biological functions. Such information can lead to the development of future anticancer therapeutics.

Differential Directional Bias in Azimuth and Elevation

Umi Keezing, Professor Frank H. Durgin

Department of Psychology, Swarthmore College
ukeezin1@swarthmore.edu

Humans overestimate their own direction of gaze in both azimuth and elevation. Prior studies indicate that the visual system expands gaze direction by factors of 1.25 in azimuth and 1.5 in elevation. The present study examines whether these differential angular gains in azimuth and elevation correspond to orientation of the observer or of the environment. In Experiment 1A, participants estimated azimuthal gaze direction in an upright virtual-reality world and in the same world rotated 90° to one side. Perceptual expansion of gaze direction was equivalent to the expected 1.25 gain in the upright world but reduced in the sideways world (provided the upright world was shown first), possibly because the sideways world appeared unrealistic. We tested the theory that directional bias depends on realism of the environment in Experiment 1B. Participants estimated azimuthal gaze direction in a realistic VR world and an abstract VR scene, and, as expected, overestimated direction less in the abstract scene.

Experiment 2 compared perceived direction in upright and sideways worlds using the same design as Experiment 1A, except now observers lay sideways, estimating directions in elevation. The sideways participants overestimated directions by a factor equivalent to the expected 1.5 gain when the world was also sideways (and the sideways world was shown first), but gave less exaggerated estimates in the upright world. This finding suggests that bias in perceived direction is more closely linked to the environment than to the observer. All in all, the environment appears to play a major role in how direction is perceived. The visual system may adjust perceived direction to the environment so as to distinguish between the directions we ordinarily see with greater sensitivity.

Functionalizing single-walled carbon nanotubes with photocleaving $[Ru(phen)_2(L\text{-}aap)]^{2+}$ as a potential mode of drug delivery

Elise Kim, Dr. Silvia Porello

Department of Biochemistry, Swarthmore College, Swarthmore, PA
ekim4@swarthmore.edu

An important focus in the ongoing development of modern medicine is finding a safe and effective method of delivering drugs to target cells. One approach that has been gaining recent attention is the functionalization of nanoparticles with therapeutically active molecules such that the nanoparticle may act as a drug carrier, working as an alternative to other methods such as distribution of the free molecule via the circulatory system, a process that can be inefficient or cause side effects[1]. Single-walled carbon nanotubes (SWCNTs) are promising candidates as drug carriers due to their large surface area and delocalized electron system, which would allow for noncovalent adsorption of potential therapeutic agents bearing polycyclic aromatic groups with extended π systems[2]. They have been evidenced to have low cytotoxicity, and using them to deliver drugs may protect the therapeutic from degradation and help localize the effects of the drug[1]. In this research, we investigated whether the metal complex $[Ru(phen)_2(L\text{-}aap)]^{2+}$, a DNA photocleaving intercalator, could be loaded onto SWCNTs and transported to target cell DNA. *Saccharomyces cerevisiae* were used as our model of a eukaryotic cell.
Our major goals for the summer were to develop a method to form the intercalator-SWCNT composite, detect binding of the intercalator to DNA *in vitro*, and compare the toxicity of the metal complexes introduced to *Saccharomyces cerevisiae* as free molecules and as intercalator-SWCNT composites.

The ruthenium(II) complex $[Ru(phen)_2(L\text{-}aap)]^{2+}$ possesses a polycyclic aromatic ligand, L-aap, which confers the potential to wrap around nanotubes via noncovalent π-π interactions, the same interactions that allow the molecules to intercalate between DNA base pairs, and photocleaves DNA upon UV irradiation. Ru-SWCNT composites were formed by tip sonicating and centrifuging a suspension of SWCNTs and Ru(II) complex, which dispersed SWCNT aggregates enough to allow Ru(II) complex to bind to the nanotube surface. Successful formation of Ru-SWCNT composites was evidenced by a visible color difference in the solution and changes in fluorescence properties. Intercalation and photocleavage was detected via fluorescence spectroscopy and gel electrophoresis, respectively, and Ru-SWCNTs were shown to exhibit intercalative and photocleaving ability comparable to those of Ru-L-aap. Toxicity studies were also performed to observe the effects of the Ru-SWCNT composites *in vivo*.

References:

1. Rastogi, V., Yadav, P., Bhattacharya, S.S., Mishra, A.K., Verma, N., Verma, A. and Pandit, J.K. (2014). *J Drug Deliv*, **2014**, 1-23
2. Huang, K., Saha, A., Dirian, K., Jiang, C., Chu, P. E., Tour, J. M., Guldi, D. M. and Marti, A. A. (2016). *Nanoscale*, **8**(27):13488-97

Effectiveness of Ultrasound and Microbubbles in Dissolving Thrombi in vitro

Hyeongmin Kim, Carr Everbach

Swarthmore College
hkim6@swarthmore.edu

In this study, we examine the effectiveness of ultrasound in dissolving human blood clots (thrombi). Thrombi narrow and clog vessels, obstructing normal flow of blood. This can instigate fatal health conditions like heart attacks and ischemic strokes. Current antithrombotic pharmacology usually affects the body systemically, which may lead to hemorrhaging if the patient has benign blood clots. This risk can be avoided by utilizing sonothrombolysis - rapid oscillations of microbubbles induced by high-amplitude pulsed ultrasound help disintegrate the mesh-like structure of blood clots. Ultrasound energy can be administered locally to a clot to avoid the lysis (breaking down) of any other untargeted, and possibly benign, blood clots. Research in sonothrombolysis helps us better understand the mechanisms behind it and form clinical applications for treating patients in a non-invasive and accurate way.

A calibrated reference hydrophone and transducer were used to identify the relevant characteristics of the sound field, such as ultrasound beam diameter, focal zone location, and magnitude, inside the experimentation tank. Human blood was collected and centrifuged to extract the plasma, which is the main constituent of the thrombi created during this study. Using the known sound field characteristics, a gelatin mold encasing the thrombus is placed in the center of the sound beam. While under sonication, another transducer detects any cavitation events that occur inside the thrombus. This detection signals the violent oscillations and collapses of microbubbles, which causes thrombolysis. For further analysis, the static pressure difference of flow inside the gelatin mold across the clot before and after sonication will be monitored to gauge the amount of blood clot dissolved away.

We intend to measure this pressure differential while sonothrombolysis is being carried out to determine the progression of thrombolysis as a function of time. Using fresh human blood samples will substantially increase the consistency of our measurements. Advances in the understanding of ultrasound-enhanced thrombolysis can help improve its clinical applications in patients, especially for those whose lives depend on rapid treatments.

The Expression and Purification of Quorum Sensing transcriptional regulator LsrR from *Escherichia coli*

Elijah N. Kissman and Stephen T. Miller

Swarthmore College, 500 College Avenue, Swarthmore, PA 19081

ekissma1@swarthmore.edu

Quorum sensing is a signal molecule dependent bacterial communication system responsible for modulating growth rates and regulating behaviors such as biofilm formation and the secretion of virulence factors. Autoinducer-2 (AI-2) is a unique quorum sensing molecule because of its presence in a wide variety of bacteria and because of its involvement in interspecies communication. The transcriptional repressor LsrR is responsible for regulating the *lsr* operon which controls the import and subsequent processing of AI-2. Previous results suggest the metabolic intermediate dihydroxyacetone phosphate (DHAP) may be directly regulating LsrR by binding to its ligand binding domain. LsrR was purified from *Escherichia coli* by cloning and expressing a previously crystallized construct containing a C-terminal hexahistidine affinity tag. Concentrating the protein for crystallization proved to be very difficult because its N-terminal DNA binding domain is very susceptible to aggregation. We will undertake several assays using the purified protein including isothermal titration calorimetry and fluorimetry to quantify the binding of DHAP to LsrR and an electrophoretic mobility shift assay to measure the effect of DHAP on the binding of LsrR to the promoter. Additionally, we will attempt to crystallize LsrR in complex with DHAP to obtain a structure of the binding pocket.

Transcription Factor Binding Site Prediction Using Neural Networks

Katherine Kwok, Keton Kakkar, Ameet Soni
Swarthmore College
Kkwok1@swarthmore.edu, kkakkar1@swarthmore.edu, soni@cs.swarthmore.edu

Transcription factors are proteins that bind to DNA to induce transcription, a biological process that converts the information stored in DNA to templates for protein synthesis. Mapping where transcription factors bind to DNA is fundamental to understanding transcriptional regulation of gene expression and interactions. The ability to predict transcription factor binding sites can also be applied to identifying drug targets for disease prevention and intervention. Typically, the transcription factor associated with each binding site can be identified by some recurring DNA sequence patterns in the site. However, transcription factor binding is influenced by other factors including the accessibility of a given DNA strand, and long-term interactions that are not captured by current methods. Consequently, this challenge necessitates an in depth and robust solution for in vivo transcription factor binding site prediction, within and across cell types. We used two different models to approach the task: a standard neural network and a convolutional neural network. Neural networks are a type of machine learning algorithm that learns abstract and hierarchical representations of data for predictive classification. Unlike the standard model, Convolutional neural networks process the input in smaller segments. Our approach is translation invariant, a property that enables efficient search for recurring DNA sequence patterns, and integrates different forms of input data, such as ChIP-seq and DNA I-seq data. We found that standard neural networks can predict transcription factor binding to DNA in one cell type and across different cell types with high accuracy. Furthermore, accuracies in across cell type binding prediction improved drastically with the inclusion of DNA I-seq data, which indicates cell-specific DNA strand accessibility.

Click Surface Modification for Controlled DNA Immobilization

Zachary D. Lamberty, Daniel K. Schwartz

University of Colorado Boulder, Boulder, CO, 80309
zlamber1@swarthmore.edu

Single molecule tracking methods have been used to investigate the diffusion and hybridization of single-stranded DNA (ssDNA) on a solid-liquid interface. These mobile ssDNA molecules are paired with complementary strands which have been covalently bound to the surface for hybridization analysis. However, previous studies have all been restricted to low concentrations of immobilized ssDNA due to the limitations of the binding reaction. Surfaces with higher concentrations of bound ssDNA probes are desirable to study due to the hope to characterize several competing density related effects, which could allow for the creation of more efficient DNA technology. Therefore, a rapid and efficient method for controlled ssDNA immobilization on fused silica surfaces was developed. First, azide functionalized silane molecules were bound to the fused silica surface, forming a monolayer. Next, strained alkyne functionalized ssDNA was reacted with the azide, forming a triazole group and bonding the ssDNA molecules to the previously formed monolayer. Control over ssDNA concentration was achieved by using polyethylene-glycol molecules to block reactive sites by engaging in a competing reaction. ssDNA molecules were successfully bound to fused silica wafers, and the control over immobilized ssDNA concentration was qualitatively verified by using total internal reflection fluorescence microscopy techniques. In addition to improving speed and efficiency when compared with previous immobilization methods, this method enables studies on the concentration-mediated hybridization times of ssDNA. This will allow for the increased study of DNA molecules, enabling us to better understand the mechanics of DNA movement and hybridization.

Response of Zooxanthellate *Aiptasia Pallida* to Flow

Elizabeth Lanphear, Rachel Merz
Swarthmore College
elanphe1@swarthmore.edu

The response of *Aiptasia pallida*, a shallow water anemone species, to velocities of flow water can be described as both passive and active. Each of these components of the response work to minimize the impact of the drag force due to flow of the water on the sessile animal. *A. pallida* boasts a symbiotic relationship with photosynthetic algae that live in its gut. The accessibility of optimal light conditions for photosynthesis as well as food capture by the anemone itself are dependent on the anemone's posturing within the flow of water. We subjected *A. pallida*, both anesthetized and sensate, to discrete velocities between 0cm/s and 50 cm/s of water in a flow tank and captured their response using a video camera. From these videos, we were able to measure the height and width of each individual at each velocity of water and to calculate the cross-sectional surface area directly exposed to flow. There was a difference between the animals that were anesthetized and those that were not. Animals that were anesthetized exhibited a kink in their body column and did not retract their tentacles to the same extent as the sensate animals that hunched over against the direction of the flow and almost completely retracted their tentacles. This difference can be attributed to some active response on part of the animal.

Functionalizing single-walled carbon nanotubes with $[Ru(bpy)_2dppz]^{2+}$ as a potential mode of drug delivery

Bo Lim (Linda) Lee, Elise Kim* and Dr. Silvia Porello

Department of Biochemistry and Chemistry, Swarthmore College, Swarthmore, PA
blee2@swarthmore.edu

With a growing number of cancer patients each year, the need for a more efficient and selective anticancer treatment is paramount. Studies show that carbon nanotubes exhibit promising characteristics, such as a large surface area that can be easily functionalized, and low cytotoxicity, essential for effective drug delivery. Single-walled carbon nanotubes (SWCNT) have a cylindrical structure consisting of sp^2-hybridized hexagonal rings, which has a delocalized electron system. Through covalent and noncovalent surface interactions, SWCNT can be "loaded" or modified with therapeutic agents. In our research, a ruthenium-based agent, $[Ru(bpy)_2dppz]^{2+}$ (bpy = 2,2'-bipyridine, dppz = dipyrido[3,2-a:2',3'-c]phenazine), a well-known DNA intercalator, was used as a cargo molecule for anticancer treatment. Our work describes the synthesis of the Ru/SWCNT composite and characterization of the the delivery of the ruthenium complex to its molecular target, DNA in vitro. Our goal is to design a composite system able to deliver its cargo (Ru complex) to cellular DNA in vivo, and study the delivery process using yeast cells.

Ru/SWCNT composites were prepared through series of sonication and centrifugation steps of solutions containing $[Ru(bpy)_2dppz]^{2+}$ and SWCNT. This step disperses the bundles of nanotubes and allows for noncovalent π-π interactions between the surface of nanotubes and the dppz ligand of the ruthenium complex. The formation of composites was detectable through UV-visible and fluorescence spectroscopy, with observed changes in MLCT and inter-ligand absorption peaks, and an enhanced fluorescence emission at 608 nm, respectively. In addition to a bathochromic shift in fluorescence spectroscopy, gel mobility assay demonstrated the delivery of ruthenium complexes from the composite to DNAs resulting in intercalation of pUC19 DNA. We have also found that photothermal treatment of Ru/SWCNT facilitates the release of cargo molecules. Our future goals include optimizing the protocol for synthesizing Ru/SWCNT composites and testing other ruthenium-based therapeutic agents, as well as studying the cellular effects of the composites.

*helped with initial acquisition of data

Saving the Best for Last: IPLS as a Capstone

Jessica Li, Professor Ben Geller

Swarthmore College
Jli1@swarthmore.edu

Physics 4L at Swarthmore is one of the many Introductory Physics for Life Science (IPLS) courses that have emerged across the country in response to a growing interest in reforming the canonical physics curriculum for life science and premedical students. The primary motivations behind this movement include: 1) to prepare students for their upper level coursework by equipping them with valuable quantitative reasoning and physical modeling skills, and 2) to promote a more engaging and positive experience with physics by harnessing their interests in their home disciplines. Although these two motivations are interrelated, they imply different prescriptions for when the course should be taken. The first suggests Physics 4L should be taken first as a foundational class; the second proposes it to be taken last as an interdisciplinary capstone, so that students will have taken other coursework that could be deepened by what they learn in physics. This poster presents our research exploring Physics 4L taken as a capstone, namely looking at how this sequence affords the advantage of connecting up students' different coursework in a meaningful and rewarding way. Using end-of-semester course evaluation data, we examine student interest scores in several life science examples encountered throughout Physics 4L. By parsing this data into students who have and have not had prior coursework, we find that students are more interested in the examples when they have taken a prior, relevant class. This result complements previous research that has found students most frequently indicate 'explanatory coherence' as their source of engagement. Taken together, this work is promising reason for Physics 4L to be taken as a uniquely interdisciplinary capstone.

Abstract: Robustness of Balanced-State Network

Victor Barranca, Han Huang, Sida Li
Department of Mathematics
Swarthmore College
Summer 2017

Temporal irregularity in the activity of neurons, usually in the form of spike-trains, is postulated to be a consequence network structure under the name "Balanced State". [Cf. Vreeswijk and Sompolinsky 1998] The explanatory power of this theory is well-investigated, but more about the robustness of this model could be explored. For instance, neurons are well-known *in vivo* to reduce their spike-frequency in the presence of a constant external stimulus. It therefore is worthwhile to ask when a such a network fails to exhibit balanced dynamics under different levels of spike-frequency adaptation. Our project explores the implication of this problem both in the original binary network and a more realistic integrate-and-fire network. Experiments demonstrate the relative robustness of balanced properties of this structure of neural network, in that balanced dynamics are preserved in various non-extreme levels of adaptation.

SETI L-band Data Recovery and Analysis

Noah Lifset, with Emilio Enriquez
UC Berkeley
nlifset1@gmail.com

Breakthrough Listen, a next generation SETI project is being conducted under the leadership of UC Berkeley. In January 2016, it began collecting data with the Green Bank Telescope in West Virginia. It started a targeted campaign with the L-band receiver (1.1-1.9 GHz). Enriquez et al. 2017 analyzed two thirds of this data comprising an homogeneous sample. The remaining one third of the L-band data taken since then is incomplete in some way, and thus required a different analysis. This project identified all possible issues with this data, and classified it based on its ability to be analyzed. Seven issues were found, and six are able to be accounted for with adapted analysis techniques. The data set consisted of observations of 366 stars within 50 pc, with 297 able to be analyzed and 69 needing to be re-observed. The Breakthrough Listen observation strategy uses 6 five minute observations per target star alternating between ON-target and OFF-target in the form ABACAD, which allows for easier radio-frequency interference identification. The analysis techniques, called *TURBO*SETI, search for a narrowband signal with a drifting doppler shift. For this data, a maximum drift rate of 4 Hz/s was chosen, which corresponds to an ET emitter on a planet three times the size of earth rotating three times as fast. An SNR threshold for signal detection of 15 was chosen, which allows for detection of signals with an EIRP (Equivalent Isotropic Radiated Power) of 9.72 $x10^9$ W for an emitter at a distance of 10 Ly. A total of 9 candidates signals were found, which were all determined to be either a satellite or another type of RFI. We can infer an upper limit of ~ 5 $x10^8$ stars in the milky way transmitting continuously towards earth in the L-band with a EIRP of 10^{12} W or greater.

Using Rhesus Monkeys to Model the Social Striatum

Jennifer Lin, Julie Fudge

Department of Neuroscience, University of Rochester Medical Center
Rochester, NY
jlin2@swarthmore.edu

In order to effectively treat psychiatric disorders, it is crucial to understand the neuroanatomy and neural circuitry of the human brain. Two important anatomical features of the brain are the striatum and the cerebral cortex, which modulate each other through a feedback loop. The striatum processes voluntary motor planning, motivation and reward. The cerebral cortex (gray matter) processes higher cognition and is divided into functionally distinct Brodmann's areas. Classical research examined striatal functioning with subjects in isolation. Recent MRI imaging research suggests, however, that the striatum may play a role in social behavior as well. There is less research on the specific neuroanatomical underpinnings of the social striatum hypothesis. Thus, the purpose of this study was to test whether cortical regions associated with social cognition directly projected to the striatum. Retrograde tracers were injected into the rhesus monkey striatum. Over a period of 10-12 days, tracer dye was taken up from the striatum to cell bodies in the cerebral cortex. The brain was then removed, sliced coronally, stained, mounted and mapped. Results showed dense populations of labeled cells in Brodmann's areas associated with social cognition, namely face and hand movement and sense of touch, the visual field, emotion processing and interoception. These findings support the presence of a neuroanatomical basis for the social striatum hypothesis. Future directions include examining distributions of labeled cells from other injection sites, studying whether the striatum is associated with hypothesized mirror neuron pathways and applying findings to biological treatments of disorders like social anxiety disorder.

Biophysical and structural studies of telomeric DNA in complex with a small molecule ligand as an anticancer strategy

(Linda) Yingqi Lin and Liliya A. Yatsunyk

Department of Chemistry and Biochemistry, Swarthmore College, PA
ylin2@swarthmore.edu

G-quadruplexes (GQ) are non-canonical secondary DNA structures implicated in cancer. Stabilization of telomeric GQ structures by small molecule ligands can serve as a novel anticancer strategy by inhibiting telomerase expression. This project explored the interaction of the ligand *N*-methyl mesoporphyrin IX (NMM) with telomeric DNA from *T. thermophile*, GGGTTGGGTTGGGTTGGG (THM), using biophysical characterization and X-ray crystal structure determination. UV-vis and fluorescence titrations revealed a 1:1 binding stoichiometry with a high binding constant of $55 \pm 35\ \mu M^{-1}$. Isothermal titration calorimetry demonstrated that the binding interaction is both exothermic and thermodynamically favorable. Diffraction-quality crystals of the THM-NMM complex were successfully obtained and X-ray diffraction data were collected at the APS synchrotron facility in Chicago. The best native data set has a resolution of 2.6 Å, but the space group remains unclear with both rhombohedral and hexagonal as distinct possibilities. Molecular replacement attempts have excellent statistics and exhibit clear electron density for the input model; however, electron density for loops and NMM is poorly defined. A brominated data set was collected at ~3.0 Å for phasing purposes. Further work towards solving the crystal structure of the THM-NMM complex will be discussed. The findings will further our knowledge of GQ-ligand interactions and inform the design of future GQ-targeting anticancer drugs.

Evolution of the *Ciona intestinalis* Heart Gene Regulatory Network

Isabel Llosa, William Colgan and Bradley Davidson

Swarthmore College PA and Friday Harbor Labs, WA
illosa1@swarthmore.edu, wcolgan1@swarthmore.edu

The basal chordate *Ciona intestinalis* has been used to untangle the chordate heart gene regulatory network because of its rapid development and compact genome. A core set of regulatory elements including *Mesp*, *FoxF*, *Hand-like*, and *GATAa* specify heart fate in *Ciona*. The enhancers for these heart genes have been characterized, but little is known about the evolution of the heart gene regulatory network. Here we characterize conserved enhancers for *FoxF* and *Hand-like* using genomic sequence from a related species, *Corella inflata*. Computational analysis revealed conserved binding sites for upstream transcription factors in both enhancers, however the order, spacing, and orientation was more highly conserved in *FoxF*. Reporter analysis demonstrated that these *Corella* heart enhancers were functional in both *Ciona* and *Corella*. Our results support evolutionary conservation of the *Ciona* heart gene regulatory network and suggest more selective constraint on *FoxF* regulation. This work also provides a framework for the identification of novel *Ciona* heart enhancers based on clustering of conserved transcription factor binding sites.

Transfecting normal human cells to express human satellite 2

Jessica Malisa and Emily Ferrari, Dawn Carone

Swarthmore College
jmalisa1@swarthmore.edu ; eferrar1@swarthmore.edu

The central dogma states that DNA is transcribed into RNA and translated into a protein product. Human Satellite 2 (HSATII) is a tandemly repeated DNA sequence that does not code for protein product. Centromeric DNA like HSATII is very difficult to study. In fact, the Human Genome Project, which was completed in 2003, was not able to map repetitive sequences like HSATII to the chromosomes. As a result, datasets have large gaps where the satellite sequences should be. HSATII is aberrantly expressed in many cancer cell types but not in normal human cells. In specific cancers, accumulation of HSATII repeats forms nuclear bodies, pulling regulatory proteins off of their target sites which leads to downstream effects and epigenetic instability. Previous efforts to transfect primary human cells and study the resulting effects of aberrant HSATII expression were unsuccessful. We worked on optimizing a transfection protocol using lipid-mediated reagent FuGENE HD to get Tig cells to express HSATII. Our initial transient transfections were successful, so we attempted two stable line transfections with antibiotic selection. Both were successful and future analysis of the stable lines will allow us to learn about the mechanisms involving HSAT II and leading to tumorigenesis.

Ultrasonic method and device for monitoring muscle water content

Colin H McLeish[1], Sergey N Tsyuryupa[2], Armen P Sarvazyan[2], and **E Carr Everbach**[1]
[1]Department of Engineering, Swarthmore College, Swarthmore, PA 19081
[2]Artann Laboratories Inc., Trenton, NJ, 08618
cmcleis1@swarthmore.edu

Background and Objective: Ultrasound velocity in soft biological tissues is defined by the molecular composition of the tissues [1]. Water is the main molecular component of soft tissues and muscle water content is typically over 70%. Ultrasound velocity in muscle is a linear function of the water content [2]. Since muscle is the main water reservoir of the human body, measurements of ultrasound velocity in muscle may serve as a means for assessment of whole-body hydration status, which is an important physiological characteristic. A compact handheld device for measuring ultrasound velocity in muscle, named "hydration monitor" (HM), was developed by Artann Laboratories to assess the water balance in muscle. The objective of this study is to test whether the HM design provides the required accuracy of ultrasound velocity measurement to estimate muscle water content variations with sensitivity on the order of 1%.

Methods: The HM uses the pitch-catch method to measure ultrasound velocity. Because the device's C-shaped probe has a fixed acoustic base, the only variable required to evaluate sound speed is the propagation time of the ultrasound pulse between transducers in a given medium.
In vitro study—Ultrasound velocity was measured in lean beefsteak (1.5x4x6.5 cm). Water injection by a syringe was used to change the sample hydration status. Water was distributed over 20 uniformly spaced injection points in the sample. Water content changes in the sample were controlled by weighing the sample.
Human study—Subject refrained from consuming liquids for 12 hours. A baseline measurement of ultrasound velocity in the soleus (calf) muscle was established. Subject consumed 1.2 L of water. Ultrasound velocity was measured at the same position every 10 minutes over 2 hours.

Results and Conclusions: Ultrasound velocity in the beef muscle linearly decreases with the increase of water content with a slope of -4.0 m/s per 1% of water content change. The dynamics of the ultrasound velocity changes in human muscle in vivo show that the equilibration of the water content following fluid consumption has time constant of about 60 minutes. The HM is capable of tracking change in total body water, shown by the trend of ultrasound velocity. The HM design provides the required accuracy of sound velocity measurement to estimate change of the sample hydration status with resolution of better than 1%, which is sufficient for measuring physiologically meaningful variations in body hydration/dehydration.
This research was partly supported by the NIH Award Number R44AG042990.

References:
1. Sarvazyan AP, Hill CR. Physical chemistry of the ultrasound-tissue interaction. In: Physical Principles of Medical Ultrasonics. Ed. Hill CR, Bamber JC, Ter Haar GR, John Wiley & Sons, 2004; Chapter 7, 223-235.
2. Sarvazyan A, Tatarinov A, Sarvazyan N. Ultrasonic assessment of tissue hydration status. Ultrasonics 43 (2005) 661-671.

Will deception work in FlipIt security games?

Do June Min, Bryce Wiedenbeck(advisor)

Swarthmore College
dmin1@swarthmore.edu

FlipIt is a security game in which two players, the attacker and the defender, compete to control a resource. Each player can perform a move that would ``flip" (a compromising attack or a reset of the system) that would yield the control of the resource. FlipIt is unique from other games that model cyber security situations in that it assumes stealthy compromise. Stealthy compromise means that neither the defender nor the attacker knows with certainty who controls the resource at any time(except the beginning), and that any move by either player is unobservable by the other.

In this study, we relaxed this assumption and allowed the attacker to play a "deceive" move, which does not compromise the system, but is indistinguishable from a normal attack for the defender. The goal of the study is to (1) characterize reasonable strategies for the attacker and the defender in this modified game, (2) determine if deceive will be played by the attacker in equilibrium, (3) if so, identify what kind of strategy deceive is played in and how much benefit it provides, and (4) finally determine if the ability to deceive allows the attacker to achieve higher payoff in some equilibria.

Using equilibrium analysis, we have found a unique equilibrium of the game, and concluded that the attacker will not play deceive in the equilibrium. In fact, we show that the attacker's ability to play deceive leads to a lower payoff, since the attacker achieves higher payoffs in some equlibria of the game with no deceive move. However, this result is limited to the instance of the game analyzed in this study, and it remains open to determine if playing deceive will be part of some rational strategy for the attacker in other variations of FlipIt security games, such as multiple-resource models.

Selecting an aptamer to bind insulin-like growth factor 1

Julia Morriss, Matthew Levy

Albert Einstein College of Medicine at Yeshiva University
jmorris2@swarthmore.edu

Insulin-like growth factor 1 (IGF-1) is a protein involved in growth and anabolism. IGF-1 levels are often measured to diagnose growth hormone disorders, as they are more stable than growth hormone levels. Existing methods of quantification of IGF-1 are costly and unable to distinguish between variants. As the first step in developing a more reliable assay LC-MS based assay for IGF-1, we sought to select an aptamer, a single-stranded oligonucleotide ligand, to bind IGF-1. We began w ith a 2'-OMe, 5-phe-dU starting library of $\sim 10^{14}$ unique sequences and completed 5 rounds of SELEX, or the Systematic Evolution of Ligands by Exponential Enrichment, a process to selectively amplify sequences that bound to our target molecule. After 5 rounds of selection our enriched library did not show binding to IGF-1. Further rounds of selection are needed to determine if any of the sequences in our library do bind but do not yet constitute a significant portion of the library to be detected.

Heterobimetallic Aluminum-Alkali Metal Complexes of New Tetra-anionic Chiral Ligands for Asymmetric Catalysis

Rares Mosneanu and Prof. Christopher Graves

Swarthmore College

rmosnea1@swarthmore.edu

Previous research in the chemistry of Al has revealed a class of heterobimetallic complexes where the Al ion acts cooperatively with an alkali-metal cation to generate a potent Lewis acid catalyst, such as Li(BINOLate)2Al (BINOL = 1,1-bi-2-naphthol). However, structural variations of the BINOLate ligand framework are difficult, limiting the ability to tune the steric profile and electronic parameters of the catalyst. We focused on the synthesis of tetra-anionic *bis*-amide-*bis*-aryloxide (ONNO) chiral ligands that can be easily varied throughout the synthetic procedure. The aluminum-alkali metal heterobimetallic complexes M(ONNO)Al (M = alkali metal cation) were prepared once we had synthesized the ligands.

We hypothesize that modifications in the structure of the M(ONNO)Al complex will lead to finely tuned acidities and steric environment at the metal ions. Once the M(ONNO)Al complexes are fully characterized (NMR and crystal structure) we will screen their catalytic aptitudes toward asymmetric organic reactions in collaboration with the Parallel Reaction Screening Service Center, in the Department of Chemistry at the University of Pennsylvania.

Zero-Diagonal Minimum Rank

Jake Mundo, Cheryl Grood, and Thomas Hunter
Swarthmore College
jmundo1@swarthmore.edu

The zero-diagonal minimum rank of graph is defined as the minimum rank of zero-diagonal matrices whose zero-nonzero pattern is given by the edges of the graph. We provide a method to characterize the graphs of zero-diagonal minimum rank less than or equal to a given positive integer. In particular, we show that the set of graphs with real minimum rank less than or equal to 4 is precisely the set of blowups of complements of line graphs of bipartite graphs. We also characterize the complete graphs having minimum rank 4 and 5 over finite fields of odd order.

Changes in hummingbird microbiome in relation to fattening cycle

Sophie Nasrallah, Sara Hiebert Burch
Isabel Erickson, Amy Vollmer

San Juan Island and Swarthmore College
snasral1@swarthmore.edu
iericks1@swarthmore.edu

Although most hummingbird species are nonmigratory, rufous hummingbirds (*Selasphorus rufus*) migrate seasonally and undergo rapid fattening in preparation for this migration. These birds follow this seasonal cycle regardless of dietary cues. In mammals, recent obesity studies have shown that weight depends on both diet and the composition of communities of microorganisms in the guts of these animals. Mice with gut microbes associated with obesity generally have less diverse microbial populations with a different representation of phyla than in lean mice. Studies show that regardless of diet, the obese mice tend to gain weight while the lean mice remain lean. When gut bacteria from lean individuals are transferred into obese mice, the obese mice become lean, suggesting that obesity is regulated in part by changes in the gut microbial population. This project explores whether changes in gut microbes play a similar role in the natural fattening cycles of rufous hummingbirds in British Columbia and on the San Juan Islands in Washington state. Fecal samples were collected from rufous and anna's hummingbirds (*Calypte anna*) that were captured for banding and measurement. Samples were sent from San Juan Island to the Swarthmore College microbiology lab for analysis. Microbial DNA from these samples was amplified using PCR and will be analyzed using Next Generation Sequencing technology to identify bacteria present in migratory (*S. rufus*) and resident (*C. anna*) hummingbirds with varying fat content. We have verified our methodology and identified three strains of bacteria present in one of our samples. However, this project will continue over the next few years and we expect to gather the bulk of our data for this study this fall. We hope that our project will contribute to the virtually unstudied area of bird gut microbes and the influence gut microbes exert on energetics and ecology, and ultimately determine whether hummingbird weight can be correlated with differences in the diversity and/or representation of gut microbe phyla.

Combining Independent Confidence Intervals to Account for Uncertain Ages in Paleontology

Jason Z. Lin, Lan Ngo, Steve C. Wang - Mathematics and Statistics, Swarthmore College

Paleontologists often want to apply quantitative methods to data representing the ages of fossil specimens. However, ages of fossil specimens are often binned to time intervals, such as the Jurassic period, rather than as an exact numerical value. This lack of precision complicates the application of quantitative or statistical methods to fossil age data. For example, a paleontologist might have two fossils that are known to date from the Triassic and Cretaceous periods, but whose exact ages are unknown. How then do we calculate means or other quantities of interest?

A common approach is for each repetition, we sample one data point from each time interval according to a Uniform distribution. Treating this randomized data set as if it were real, we apply some method to arrive at a confidence interval (CI). Repeating m times generates m CIs, each estimating the parameter of interest θ independently. A natural question to ask is: how can we combine the m CIs to arrive at a single CI with a desired confidence level?

Our approach builds on a procedure first used by Marshall (1995) to estimate the time of the end-Cretaceous mass extinction using confidence intervals on stratigraphic ranges for multiple taxa, and later generalized by Wang and Marshall (2004) for the same situation.

Utilizing Statistical Analysis to Develop a Python Algorithm to Constrain Orbits of Young Binary Systems

Natasha Nogueira, Professor Eric Jensen

Swarthmore College
nnoguei1@swarthmore.edu

Measuring the orbits of young binary systems can provide the stars' individual stellar masses and insight into the dynamical effects they should have on each others' protoplanetary disks, as well as form a better understanding of stellar formation of young, low mass, binary stars. As a byproduct of our ALMA observations of disks in young binary systems in the Taurus star-forming region, we are developing a Python program that improves constraints on binary orbital parameters through a Bayesian analysis. While the coverage of our observed systems is $< 5\%$, resulting in an indefinite orbit, our goal is to improve the algorithm to predict distributions of orbital parameters within a certain error range. Binary systems with resolved, definite orbits were used to test the algorithm.

This work makes use of the following ALMA data: ADS/JAO.ALMA#2011.0.00150.S. and ADS/JAO.ALMA#2013.1.00105.S. ALMA is a partnership of ESO (representing its member states), NSF (USA) and NINS (Japan), together with NRC (Canada) and NSC and ASIAA (Taiwan), in cooperation with the Republic of Chile. The Joint ALMA Observatory is operated by ESO, AUI/NRAO and NAOJ. The National Radio Astronomy Observatory is a facility of the National Science Foundation operated under cooperative agreement by Associated Universities, Inc.

Stabilizing the G-quadruplex form in VEGF and G4TERT sequences

Samantha T. Nyovanie, Liliya A. Yatsunyk

Swarthmore College, PA
snyovan1@swarthmore.edu

The folding of guanine-rich DNA sequences into G-quadruplex (GQ) structures has been a growing field of interest and research since the discovery that these structures could inhibit growth of cancer cells. DNA sequences with GQ-forming potential are overly abundant in telomeres and in promoters of oncogenes, which establishes GQs as a prospective anticancer target. A GQ structure is formed by the π-π stacking of multiple G·G·G·G tetrads, in which guanines are held together by Hoogsteen hydrogen-bonding. The research in the Yatsunyk lab is aimed towards solving GQ crystal structures and exploring ligand interactions with GQ DNA. VEGF and G4TERT are some of the G-rich DNA sequences that are currently studied in the lab. VEGF sequence is found in the promoter region of the vascular endothelial growth factor gene, which is upregulated in a variety of cancers and promotes growth of cancer cells. G4TERT sequence is found in the promoter region of hHERT gene, which encodes for the catalytic domain of human telomerase, and promotes cancer cell survival. This study investigates the conditions that best stabilize the GQ form of these sequences, by determining the suitable buffer and designing variants extended with additional nucleotides. The stability of the GQ is evaluated by circular dichroism (CD) and UV-vis spectroscopies, and its conformational homogeneity is analyzed by PAGE gel electrophoresis. By stabilizing GQ formation in VEGF and G4TERT, the proliferation of cancer cells could be minimized. The structure of GQ DNA, once obtained, could be used in *in silico* drug screening for quick and efficient identification of the potent cancer therapeutics.

Pitch and Helical Twisting Power Measurements in Chiral Chromonic Liquid Crystals

Timothy Ogolla, Peter Collings

Swarthmore College
togolla1@swarthmore.edu

The recent interest in lyotropic chromonic liquid crystals (LCLCs) has resulted in significant understanding of the assembly behaviour and liquid crystal properties of these water-based systems. On the other hand, there has been much less investigation into chiral LCLCs, which result if the chromonic molecule is chiral or if a chiral dopant is added to the solution. Measurements of the pitch of the LCLC disodium cromoglycate (DSCG) with several chiral dopants using both the Cano wedge and fingerprint texture methods are reported. The results include quantitative measurements of both the pitch and the helical twisting power. The ability of dopants to induce twist in DSCG varies widely, with some having almost no effect, with others producing a pitch approaching 3 μm and with most displaying an inverse pitch–dopant concentration dependence that is nonlinear at high concentrations.

Investigating the soil mycorrhizal fungal community composition of invasive plant species in the Crum Woods

Bennett Parrish, Amy Vollmer, José-Luis Machado

Swarthmore College
bparris1@swarthmore.edu

Invasive plant species are considerable threats to native ecosystem structure and function. The interaction between these plants and soil fungal communities plays a significant role in determining above ground biodiversity. Accordingly, changes in the fungal community composition of soils colonized by invasive plant species may greatly affect ecosystem function and native plant community composition. Earlier research suggests that invasive plant species can adversely affect the fitness of native species through alterations of the chemical composition of the soil and also have produced major shifts in the composition of the rhizosphere microbial communities as invasive plant species colonized new areas. However, little is currently known about the effect of invasive plant species on soil fungal composition. Additionally, fungal regulation of litter decomposition and nutrient cycling in terrestrial ecosystems is likewise under-researched considering that fungi are the primary decomposers of dead plant biomass in terrestrial ecosystems. This research project will document the rhizosphere fungal communities found in the soils occupied by invasive Norway maple (*Acer platanoides*) and compare their composition with corresponding native Sugar maple (*Acer saccharum*) found in the Crum Woods. The current emergence of high throughput sequencing as a fast and affordable technique makes this project feasible. Protocols for DNA extraction, 18S Illumina Amplicon, and QIIME processing that are part of comprehensive guide for sequencing soil fungal communities compiled The Earth Microbiome Project. Identifying the characteristics of soil fungal communities associated with invasive plant species will provide insight into the impact of invasive species on nutrient cycling, leaf litter decomposition, and possible feedbacks to climate change.

We would like to acknowledge the Swarthmore College Department of Biology Enders Research Memorial Award for supporting funding for this project.

Examining the structural and functional properties of the *Thermobacillus composti* ortholog of autoinducer-2 receptor LsrB

Nicholas Petty, Stephen Miller

Swarthmore College
Npetty1@swarthmore.edu

However, studies have shown that bacteria can communicate with eachother, both within and between species, through a process known as quorum sensing. One such mechanism is known as the *lsr* rpathway and is present in many clinically relevant species of bacteria including *E. coli* and *S. typhimurium*. The *lsr* pathway in particular has drawn interest for its role in biofilm formation, bioluminescence, and the secretion of virulence factors. This study focused on one of several proteins comprising the Lsr pathway, LsrB. LsrB is the surface receptor protein of the Lsr pathway, accepting the signaling molecule, autoinducer-2 (AI-2), and facilitating its transport into the cell. In particular, I focused on *Thermobacillus composti* LsrB, which only shares 17% sequence identity with canonical *S. typhimurium* LsrB. With *T. composti* LsrB sharing such a low sequence identity with other strains, its identity as an LsrB protein needed to be confirmed. A combination of functionality assays and structural analysis elucidated whether *T. composti* LsrB binds AI-2. I used a bioluminescence assay to qualitatively assess AI-2 binding. This assay involves the use of the bacteria *Vibrio harveryi*, which bioluminesces in the presence of AI-2. The assay showed that *T. composti* LsrB induced luminescence in *V. harveyi*, indicating AI-2 binding. After demonstrating AI-2 binding, I took steps towards crystalizing *T. composti* LsrB. Initial attempts at crystallization have worked with a trypsin cut LsrB variant. Crystallization trials are still in early stages and refinements are being made to promising conditions.

Streptococcus pyogenes activates sensory neurons to release CGRP, inhibiting neutrophil killing

Makayla Portley, Felipe Ribeiro and Isaac Chiu

Harvard Medical School
mportle1@swarthmore.edu

Streptococcus pyogenes, known to cause a variety of painful conditions ranging from strep throats to necrotizing fasciitis, is a bacterium whose virulence factors are being thoroughly explored. "Pain out of proportion" with other clinical findings is a hallmark of necrotizing fasciitis, the most invasive and life-threatening disease caused by *S. pyogenes*. In this work, we show that intense pain is not just a symptom but also a virulence mechanism of invasive *S. pyogenes* infections. We observed previously that *S. pyogenes* directly activates nociceptor sensory neurons to cause pain and also to induce the release of calcitonin gene-related protein (CGRP) from peripheral nerve endings.

We performed co-culture *in vitro* experiments using isolated mouse and nociceptor neurons from dorsal root ganglion (DRG) to reveal the interactions that occur between these cells and the impact of that on the capacity of neutrophils to kill *S. pyogenes*. We observed that the presence of mouse DRG neurons inhibit neutrophil killing of bacteria, and that these effects can be reversed using CGRP antagonists or BoNT/A (inhibits neuropeptide release). CGRP agonist alone also reproduced the effects of DRG neurons on the capacity of neutrophil to kill *S. pyogenes*. Confocal images comparing vehicle and CGRP-treated conditions revealed a difference not in the number of neutrophils containing bacteria, but in the concentration of bacteria within the cells. In CGRP treatment conditions, the bacteria within neutrophils appeared to not only survive, but thrive, reproduce, and, in some cases, escape into the cytoplasm, revealing a mechanism for potentially furthering infection. The inability to CGRP-exposed neutrophils to kill GAS could be due to a variety of mechanisms, which remain to be investigated. These data demonstrate that *S. pyogenes* activates nociceptor neurons during infection to release neuropeptide that increase its resistance to neutrophil killing.

Where's The Junk?: Mapping HSATII in the Human Genome

Rajiv Potluri, Dawn Carone Ph.D.

Swarthmore Department of Biology, 500 College Ave, Swarthmore PA 19081
rpotlur1@swarthmore.edu

Although the Human Genome Project has been deemed complete, there are still gaps in the centric and pericentric regions of current human genome assemblies (Kent et al., 2002). In these chromosomal regions, this is due to the extreme difficulty in mapping the tandemly repetitive sequences harbored there. These centromeric satellites are defined by their sequence monomers into alpha SAT, HSATI, HSATII, and HSATIII. The focus of our research, HSATII is a highly conserved, 24-bp, tandemly repeated sequence present on only a subset of chromosomes in the human genome (Tagarro et al., 1994). Recent work has defined HSATII and HSATIII sequence into sequence subfamilies (Altemose et al., 2014). Within HSATII, they were able to define three unique oligomers: HSATII A1, HSATII A2, and HSATII B (Altemose et al., 2014). Utilizing these new subtypes of HSATII, we attempted to create the first chromosome-specific map of HSATII sequence in the human genome. We performed a combination of *in silico* analysis of single-reference genome assemblies from the National Center for Biotechnology Information (NCBI) and fluorescent *in situ* hybridization (FISH) of human primary fibroblast chromosomes with HSATII oligomers to successfully create a cytogenetic map of the three HSATII subfamilies in the human genome. We observed chromosome-specific differences in the presence of each HSATII oligomer, supporting the hypothesis that unique, chromosome-specific HSATII sequences exist in the human genome. Of particular import is the unique presence of the HSATII A1 sequence on chromosome 11, as well as HSATII B sequence on chromosome 3. In addition, we found that chromosome 7-specific HSATII sequence contained mostly A2 sequence, corresponding with RNA FISH data in cancer cells suggesting that the A2 sequence is aberrantly expressed from chromosome 7 (Hall et al., 2017).

Efforts towards the Crystal Structure of a Noncanonical DNA Repeat Implicated in Cancer

Barrett Powell,[a] **Jessica Chen**,[a] **Deondre Jordan**,[a] **Eric Brown**,[b] **Liliya A. Yatsunyk**[a]
[a]*Dept. of Chemistry and Biochemistry, Swarthmore College, 500 College Ave., 19081 Swarthmore, United States*
[b]*Dept. of Cancer Biology, Perelman School of Medicine, University of Pennsylvania, 421 Curie Blvd., 19104, Philadelphia, United States*
bpowell1@swarthmore.edu

Certain intrinsically difficult-to-replicate DNA sequences are associated with replication stress, which can lead to cancer-causing mutations. Extensive bioinformatics studies of the mammalian genome identified a variety of such sequences, many of which constitute centrally positioned DNA tandem repeats. This work focuses on one of them, $(CAGAGG)_n$. Based on a variety of biophysical techniques including circular dichroism (CD), UV-vis, ^1H NMR, AUC, and gel electrophoresis, we suggest that $(CAGAGG)_n$ folds into an unknown structure that does not fall into any currently known category of DNA motifs (e.g. duplex, triplex, guanine quadruplex, i-motif, etc). Inspired by the similarities in CD spectra with a non-canonical DNA structure from Plavec's laboratory, we hypothesize that the $(CAGAGG)_n$ repeats form stacked planar G-C-G-C elements (either a tetrad or adjacent base pairs) connected by AGAG loops in an overall antiparallel conformation (**Fig. 1**). In addition to extensive biophysical verification of this model, our current effort has been to crystallize this sequence in order to solve its 3D structure via X-ray crystallography. We have pursued a wide array of approaches to establish a suitable oligonucleotide for crystallization, including crystallizing constructs of various lengths and frame shifts and co-crystallizing with nondisruptive and stabilizing ligands. Recently, we have designed small targeted modifications to the repeat sequence in order to increase its stability and to encourage favorable crystal packing. We used PAGE gel electrophoresis and CD spectroscopy to verify viability of new constructs for crystallization and their structural consistency with the native sequences. Crystallization results will be discussed.

Irrelevant speech suppresses verbal rehearsal

Morgan Purcell and Christina Labows, Lisa Payne
Selective Attention Lab, Swarthmore College, Swarthmore, PA

The irrelevant speech effect is a reliable decrease in accuracy of serial recall when background speech is played during silent verbal rehearsal of a memory set of words. Both fMRI and PET studies have shown reduction in neural activity in left-lateralized frontotemporal regions during the irrelevant speech effect, leading to the assumption that irrelevant speech suppresses neural activity related to maintaining the information relevant to the task. When ignoring sensory stimuli is beneficial to a task, suppression of neural activity related to these stimuli has been reflected by an increase in alpha oscillations (8-14 Hz) in the sensory cortex. If suppression of verbal rehearsal during irrelevant speech occurs via the same mechanism, alpha oscillations should increase in left-lateralized frontotemporal areas of the brain associated with rehearsal. In this study, participants were briefly presented a sequence of five words and then instructed to internally rehearse these words during a four second retention period, until directed to recall the words out loud in the order they had been presented. Throughout the retention period, participants heard either white noise (as a control) or sound clips of irrelevant speech. Consistent with the irrelevant speech effect, participants were less accurate in recalling words when they heard irrelevant speech than when they heard white noise. In addition, EEG results showed a relative increase in alpha oscillations in left-lateralized frontotemporal regions during the retention period for trials with irrelevant speech as compared to white noise trials. This indicates that irrelevant speech suppresses a person's internal verbal rehearsal even when attending the internal rehearsal is beneficial to the person's current task. This bottom-up mechanism of suppression in frontal regions of the brain adds to support of alpha oscillations as a possible inhibitory mechanism of suppression in areas beyond the sensory cortex.

Analysis of the Spread of Vector Borne Diseases with Delay Differential Equations

Yusuf Qaddura, Advisor: Nsoki Mavinga

Swarthmore College
yqaddur1@swarthmore.edu

We model the spread of vector borne diseases (e.g. Zika Virus and Malaria) using a two-lag delay differential equation. We study local stability of equilibria and simulate numerical solutions using MATLAB. Moreover, we discuss the boundedness and positivity of solutions.

The model is an extension to another previously studied one by Cooke [1] who considers an incubation period (delay) in vectors only. We modify his model by adding a human incubation (delay) period and an assumption on the size of the exposed human population. We show that there are some values of transmission and recovery rates for which the reproduction number of the disease is less than one so that the disease dies out. On the other hand, we show that the disease spreads into an endemic when the reproduction number is greater than one for other values of transmission and recovery rates. In addition to that, we observe, through MATLAB simulations, that the solution could possess chaotic behavior and sometimes unboundedness.

Literature Cited:

1. Kenneth L. Cooke (1979): *Stability Analysis for a Vector Disease Model*. Rocky Mountain Journal of Mathematics, Vol 9, Number 1.

Investigation of the therapeutic potential of combining CDK7, CDK12/13, and BET inhibitor strategies in Small Cell Lung Cancer

Alexandra R. Rabin, Camilla L. Christensen Ross, PhD.

Dana Farber Cancer Institute, Boston, MA
arabin1@swarthmore.edu

Small cell lung cancer (SCLC) affects 10-15% of lung cancer patients. Of all lung cancer subtypes, SCLC is particularly challenging to treat; the disease is often detected in its later stages, resulting in a five-year patient survival rate of 6%. Considering the poor prognoses of almost all SCLC patients, including those treated with standard chemotherapy and radiation, a novel treatment strategy is necessitated. Targeted therapies have emerged as a potential approach to SCLC treatment. Among these, novel drugs that target cyclin-dependent kinases (CDKs) have been found to be effectual in a number of cancer subtypes, including SCLC. It has been found that certain targeted therapies can be more effective when employed in concert with inhibitors directed at other tumor-related proteins. Of particular interest are potential opportunities for interaction between these CDK inhibitors, with roles including cell-cycle and DNA repair regulation, and drugs that inhibit either other members of the CDK protein family or the Bromodomain and extraterminal (BET) domain family, among other prospects for synergy. Here, we investigate two potential combinations of these inhibitors, examining whether these drugs exhibit effective synergy between CDK7, CDK12/13, and BET *in vitro*. To assess the synergy of the CDK and BET inhibitors, we performed a series of five-day cell viability assays and compared the resultant IC50 results, using standard SCLC chemotherapy (Cisplatin and Etoposide) as a benchmark for efficacy. We found that the novel CDK7 inhibitor used was particularly potent, as evidenced by a similar IC50 value between the inhibitor alone and in combination with both the CDK12/13 and the BET inhibitor. This suggests that the potential effects of synergy between multiple inhibitors were precluded by the overwhelming efficacy of the CDK7 inhibitor. We also performed a number of cDNA analyses using quantitative PCR to determine the intracellular effects of treatment with a number of these novel inhibitors. Future directions include further investigation of the downstream effects of potentially-synergistic drug combinations. This would potentially elucidate the feature of the particularly aggressive CDK7 inhibitor preventing other drugs from acting synergistically within the tumor cell. Additionally, as this study was carried out solely *in vitro*, we will treat mice with these drugs and drug combinations to assess their efficacy *in vivo*.

Characterization of Silver Nanoparticle Behavior via Electrochemical and Spectroscopy Analysis

Arka Rao '18, Laela Ezra '19, Kathryn Riley
Swarthmore College
lezra1@swarthmore.edu, arao2@swarthmore.edu

The use of nanomaterials for a range of environmental, medicinal, and commercial applications has dramatically increased in recent years. However, the release of these materials into the environment has raised concern over their potential harmful effects necessitating the development of in situ tools for nanomaterials characterization. Here we describe the development of electrochemical and spectroscopic techniques for characterization of spherical silver nanoparticles (AgNPs). Differential pulse stripping voltammetry (DPSV) is a sensitive electrochemical technique for the detection of metal ions and is well-suited for investigation of nanomaterial dissolution properties. DPSV studies of the dissolution of silver ions from AgNPs prepared in simulated sweat solutions with differing pH and salt concentrations will be presented. It was found that more acidic solutions resulted in a higher level of dissolution. In addition to dissolution, AgNPs undergo aggregation in saline solutions, which is dependent both on particle size and salinity of solution. At certain salt concentrations, a critical coagulation concentration (CCC) is obtained and the particles aggregate. AgNPs have peak absorbances between 390 to 500 nm, which can be monitored to observe changes in particle dispersion. Using UV-Vis spectroscopy, aggregation kinetics were measured for AgNPs at varying pH and salt concentration.

Structural Studies of the Influenza A M2 Membrane Protein Critical to Viral Budding and Genome Packing

Hayley Raymond, Abigail Wong-Rolle, and Kathleen P. Howard

Department of Chemistry and Biochemistry, Swarthmore College, Swarthmore, PA 19081
hraymon1@swarthmore.edu

Influenza A is a virus that is highly pathogenic and causes pandemics. The membrane-bound M2 protein plays a critical role in the viral life cycle and is a potential target for the development of antiviral drugs. Residues 60-70 of the C-terminal domain of the protein are previously structural uncharacterized but are known to facilitate viral genome packing and may contain a general binding site for another influenza A protein, M1. We used site-directed spin label EPR (SDSL-EPR) spectroscopy to probe the structure, mobility, dynamics, and membrane topology of full-length M2 in this region. Continuous wavelength (CW) spectra revealed that moving outward from the transmembrane domain, residues display increased mobility, with the most pronounced increase in mobility around residues 64-65. Power saturation data in the presence of paramagnetic relaxation reagents oxygen and nickel (II) ethylenediaminediacetate (NiEDDA) revealed that the region is associated with the cell membrane but extends towards the aqueous phase, with a significant tilt away from the membrane at a point around residues 64-65.

The role of the cytoskeleton in FGFR trafficking in *Ciona intestinalis*

Elijah Reische, Brad Davidson

Swarthmore college
ereisch1@swarthmore.edu

During embryonic development, dividing cells are exposed to a wide array of signaling pathways and external cues that work to determine cell fate. While a heart founder cell is dividing in a developing embryo of *Ciona intestinalis*, a marine tunicate, a membrane protein called fibroblast growth factor receptor (FGFR) is trafficked within the cell during division, resulting in a ventral membrane domain that is enriched with FGFR. After completion of mitosis, the daughter cell that inherits this FGFR-enriched membrane domain will become a heart progenitor, and the other daughter will become an anterior tail muscle cell.

The exact processes that underlie this redistribution remain poorly characterized. I attempted specifically to clarify the role of microtubules – long, thin structures involved in intracellular transport and mitotic coordination – in FGFR trafficking during heart founder cell mitosis. To do this I treated developing embryos with nocodazole, a reversible microtubule-destabilizing drug, just before their heart founder cells divided.

Confocal microscope images showed that embryos treated with nocodazole had a different distribution of FGFR than control embryos, with more FGFR in the periphery of the cell and less in the deep interior. These results indicate that microtubules may be involved in some capacity in bringing FGFR from the membrane to the interior of the cell. It is possible that dynein, a motor protein that moves directionally along microtubules, is responsible for trafficking FGFR inside the cell and that microtubules are necessary to provide a path for this process. Further investigations should be performed to clarify the exact role of dynein in FGFR trafficking, as well as to investigate the activity of other cytoskeletal elements, such as actin and myosin.

Relative contributions of mammal and habitat on dung beetle community structures across a deforestation gradient

Jordan Reyes, Elizabeth Nichols

São Paulo, Brazil
Jreyes4@swarthmore.edu

Dung beetles are both sensitive to changes in mammal community structure (via altered fecal resource availability), and to habitat loss- via direct effects on altered microclimate, and indirect effects on mammal communities. Partitioning the relative impacts of these two drivers of decline in dung beetles in real landscapes remains uncharacterized to date. We examined the relationships between dung beetle response to both native forest loss and changing mammal communities using a well-replicated landscape-scale analysis in the Brazilian Atlantic Forest. We used generalized multilevel path analysis (GMPA) to quantify dung beetle abundance responses to both native habitat loss and mammal occurrence. We found that dung beetles are not impacted directly and independently by forest loss, but rather through the combined indirect effects of deforestation and changing mammal communities.

CMB Constraints on Spatial Anisotropy of the Fine-Structure Constant

David Robinson, Davy Qi, and Professor Tristan Smith

Swarthmore College
drobins4@swarthmore.edu, yqi1@swarthmore.edu, tsmith2@swarthmore.edu

In this project, we use observations of the cosmic microwave background (CMB) data from the *Planck* satellite to constrain the spatial variation of the fine-structure constant. The fine-structure constant is a fundamental constant of physics that controls the strength of electromagnetic interactions. The physics of the CMB relies on the exact value of the fine-structure constant, leading to a particular set of effects if it were to vary in space. This work is the first to consider how a variation in the value of the fine-structure constant will affect estimates of the lensing potential power spectrum from the CMB trispectrum (four-point correlation function). We compute all of the effects of the variation of the fine-structure constant on the CMB and lensing potential estimates and use a Markov Chain Monte Carlo analysis to compare them to the data. We find that with this data the fractional variation of the fine-structure constant must be less than 4.2×10^{-3} (at 95% confidence level). This improves upon previous work which used a different technique and an older dataset and found an upper limit of 6.8×10^{-3}.

Acceleration and Compression of Taylor State Plasmas on SSX

Jaron Shrock, Dr. Mike Brown

SSX Lab, Swarthmore College
Jshrock1@swarthmore.edu

In the Swarthmore Spheromak Experiment (SSX), compact toroidal plasmas are launched from a coaxial plasma gun and evolve into minimum energy twisted Taylor states. The plumes initially have a velocity ~ 40$ km/s, density ~ 0.4×10^{16} cm^{-3}, and proton temperature ~ 20 eV. After formation, the plumes are accelerated by pulsed pinch coils with rise times $\tau_{1/4} = (\pi/2)\sqrt{LC}$ less than 1 μs and currents $I_{peak} = V_0/Z = V_0/\sqrt{LC}$ on the order of 10^4 Amps. The accelerated Taylor States are abruptly stagnated in a copper flux conserver, and over the course of $t < 10$ μs, adiabatic compression is observed. The magnetothermodynamics of this compression do not appear to be dictated by the MHD equation of state $\frac{d}{dt}\left(\frac{P}{n^\gamma}\right) = 0$. Rather, the compression appears to evolve according to the Chew-Goldberger-Low (CGL) double adiabatic model. CGL theory presents two equations of state, one corresponding with particle motion perpendicular to magnetic field in a plasma, the other to particle motion parallel to the field. In preliminary non-accelerated experiments, we observe Taylor state compression most in agreement with the equation of state derived from the parallel equation of state: $\frac{d}{dt}\left(\frac{PB^2}{n^3}\right) = 0$.

Pediatric Second Primary Thyroid Cancer: Epidemiologic Characterization & Radiation Implication

Casey Lu Simon-Plumb, advised by: Ruth Montesines and Dr. Lauren Holmes Jr.
A.I. duPont Hospital for Children Office of Health Equity and Inclusion
csimonp1@swarthmore.edu

Childhood radiation exposure has been linked to thyroid cancer because radiation is a known carcinogen and both the thyroid gland itself and children, due to biology during development, are acutely radiosensitive. In this retrospective cohort study, the study population comprised children diagnosed with thyroid cancer between 1973 and 2013, age 0-19 years in the Surveillance, Epidemiology and End Results (SEER) registry. Annual percent change (APC) over 5 year intervals was used to analyze incidence rate trends and a binomial regression model was applied to examine the hypothesis that radiation has an effect on the development of SPTMs. SPTM incidence has increased in recent years, with the last 10 years accounting for 66.66% of diagnoses. Our multivariable binomial regression found that compared to whites, blacks were 60% less likely and others races/unknown race were 18% more likely to develop SPTMs. Along with this, women were 63% less likely to develop SPTM and those residing in urban and rural areas, compared to metropolitan regions, were more likely (31% and 66% respectively) to develop a SPTM. Our results point to the importance of further research looking at the drivers of SPTM health disparities among sex, race and location as well as more sensitive analysis of incidence trends in the last five years and radiation type and dosage in SPTM risk.

Using Neural Approximations to Solve Games

Sam Sokota, Bryce Wiedenbeck

Swarthmore College
ssokota1@swarthmore.edu

Our research is focused on using neural function approximation to find epsilon Nash equilibria in stochastic games. We are attempting to improve existing means of doing so by devising an efficient means of calculating the Nash equilibria of stage games. To this end, we use deviation payoffs, a concept termed by Professor Wiedenbeck referring to the expected payoff to a player for deviating from the mixed strategy that is being played by the player's opponents. To learn the deviation payoffs, we generate a representative set of mixed strategies. From each of these mixed strategies, we sample a set of actions. Finally, we observe the payoff of each allowed action against the set of sampled actions. These observed payoffs are an unbiased estimation of the true deviation payoffs. Using this data, we train a neural network to approximate the function from mixed strategies and actions to deviation payoffs. There are several existing equilibria finding algorithms that, when provided a precomputed deviation payoff function, can efficiently calculate Nash equilibria. In stochastic games with correlated stage games, we can use one neural network to learn the deviation payoffs of many stage games, taking advantage of the correlation between stage games to generalize. We are now considering larger algorithms designed to calculate the Nash equilibrium of an entire stochastic game that could use our stage game equilibria computation as a sub process.

As a precursor to our current research, we replicated the work done by Heinrich et al. in *Fictitious Self-Play in Extensive-Form Games* and *Deep Reinforcement Learning from Self-Play in Imperfect-Information Games*. In these papers, Heinrich et al. extended fictitious play, an algorithm for calculating Nash equilibria in zero-sum stage games, to extensive-form games, and created a neural approximation of this extension. The authors demonstrate the effectiveness of this neural approximation on several poker games. We achieved similar results to those reported in the papers for Leduc Hold'em.

Biofuels at Swarthmore

Sierra Spencer, Carr Everbach, The Stone House Group

Swarthmore, PA
Sspence1@swarthmore.edu

Biofuels were researched as part of Swarthmore's greater Energy Strategy for Sustainability and Resiliency and in contributing to the college's goal of reaching carbon neutrality by 2035.The sustainability and environmental impact of biofuels were assessed, and based on the classification by higher education organizations, such as Second Nature, of biofuels as carbon neutral, the lifecycle lens of viewing carbon emissions was legitimized. Gross emissions of different biofuels and usage scenarios were estimated and compared to Swarthmore's current emissions from natural gas. From preliminary comparisons of biomass-based biofuel, soybean-derived biodiesel, and waste cooking oil-derived biodiesel, the waste vegetable oil-derived biodiesel was determined to be the best fit for Swarthmore given its "drop-in" nature, ability to be used with Swarthmore's current heating equipment for natural gas, and availability from vendors. Biodiesels also seem to have less gross emissions of major pollutants, as long as 100% biodiesel is used, as opposed to a blend. Many local vendors, however, only provide up to a 20% blend of biodiesel, therefore reducing the environmental advantages that would be reaped from sourcing biodiesel from most local vendors. Boston-based Lifecycle Renewables, however, provides 100% biodiesel that is derived from waste cooking oil collected from Boston-area restaurants and food manufacturers. Users of Lifecycle Renewables' heating biodiesel product, LR100, such as Keene State College, have not reported any issues with many of the logistics, fuel performance, or equipment function that Swarthmore was concerned about. Lifecycle Renewables, along with most other providers contacted, participate in the RIN market, which helps to make biofuels and biodiesels more cost competitive. More price information on biofuels and biodiesels available is necessary for a more comprehensive cost assessment. The potential to use Swarthmore's own waste cooking oil was investigated, but after a recent switch in oil management companies and the relatively small scale of waste oil produced, initial findings reveal that this would not be feasible or cost-advantageous over the long-term. Storage and logistics were researched and varied depending on the type or vendor of biofuel, but the acidity of biomass-based biofuel poses several significant storage and equipment function challenges. The permitting process also varies based on the type of biofuel or biodiesel, and the first step in determining approval or further steps required is submitting emissions estimates in the Pennsylvania DEP's Request for Determination. This project will continued to be researched throughout this academic year during my Presidential Sustainability Research Fellowship and potentially through my E90 project.

Investigation of Sema6a Reverse Signaling and the Role of Secreted Sema6a Signaling

Elizabeth Stant, Alicia Eberts

University of Vermont
estant1@swarthmore.edu

During eye development, the eye field separates from the blastula to form bilateral vesicles that then will evaginate from the forebrain. One of the molecular mechanisms that keeps these eye fields cohesive during this time of extensive cell migration and proliferation is repulsive signaling from the ligand Sema6A (Ebert et. al, 2014). Sema6a, located in the eye vesicle, is known to interact with Plexna2, located in the ventral vesicle, through a forward signaling sequence where Sema6a acts at the ligand and Plexna2 as the receptor. What we sought to investigate here was the potential role that Sema6a has in reverse signaling, as well as what proteins and phosphorylation sites help regulate eye development on its intracellular domain. Through trial and error, we found that the Sema6a antibody was not optimized to work well for western blotting and immunofluorescence, which led us to a cloning project to help improve results of future experiments involving Sema6a signaling. This cloning project involved creation of a Flag-tagged Sema6a DNA, which would make the protein easier to study as the Flag antibody was able to successfully identify Flag-tagged PlexinA2 in the cell. PCR techniques were used to create two forms of the Flag-tagged Sema6a protein, one with its intracellular domain and one where primers were used to remove its intracellular domain. By having these two forms of the protein to study, we could understand more about the importance of the role Sema6a's intracellular domain plays in a reverse signaling pathway.

Further, after discovery by the Ballif/Ebert lab of a naturally secreted Sema6a found in HEK-293 cells, we sought to understand the potential role that protein could play in maintaining eye cohesion. Eye explants of 18 somite RX3 GFP zebrafish were placed in both two different types of culture medias, one with the naturally secreted Sema6a and one with mock media. Comparison of the eye explants after six hours in the media showed that the eyes in the secreted Sema6a media contained an eye cup and had little ectopic neurons, while those in the mock media had ectopic branching outside of the eye. This finding indicate that secreted Sema6a plays an important role in repulsive signaling for eye cohesion.

Precision Electron Density Measurements in the SSX MHD Wind Tunnel

E. M. Suen-Lewis, M. Kaur, D. A. Schaffner, M. R. Brown

Swarthmore College
elewis1@swarthmore.edu

We characterize fluctuations of the line averaged electron density of Taylor states produced by the magnetized coaxial plasma gun of the SSX device using a 632.8 nm HeNe laser interferometer. The analysis method uses the electron density dependence of the refractive index of the plasma to determine the electron density of the Taylor states. Typical magnetic field and density values in the SSX device approach about B = 0.3 T and $n = 0.4 * 10^{16}$ cm^{-3}. Analysis is improved from previous density measurement methods by developing a post-processing method to remove relative phase error between interferometer outputs and to account for approximately linear phase drift due to low-frequency mechanical vibrations of the interferometer. Precision density measurements coupled with local measurements of the magnetic field will allow us to characterize the wave composition of SSX plasma via density vs. magnetic field correlation analysis, and compare the wave composition of SSX plasma with that of the solar wind [1]. Preliminary results indicate that density and magnetic field appear negatively correlated.

[1] G. G Howes et al., *The Astrophysical Journal Letters*, vol. 753, July 2012.

Innate Immunity Interactions in *Aiptasia pallida*

Serena Sung-Clarke, advised by Elizabeth Vallen
Swarthmore College
ssungcl1@swarthmore.edu

Coral reefs are extraordinary ecosystems; they take up less than one percent of the ocean, and yet, they are home to an estimated 25% of the marine life on the planet. Because of rising sea temperatures and ocean acidification, the corals that form the basis of these ecosystems are under direct threat. Coral polyps have an important symbiotic relationship with photosynthetic algae, called zooxanthellae, which will live inside the cells of the coral. The zooxanthellae can photosynthesize, providing the coral with most of its energy needs, and the coral provides the zooxanthellae with nutrients. Under stressful conditions, however, the polyp will expel the zooxanthellae. Given enough time without its symbionts, the coral eventually dies – and on a larger scale, this is called coral bleaching.

The cellular process behind this ecologically relevant phenomenon is still not well understood. Corals live in complex environments, surrounded by potentially beneficial symbionts and harmful pathogens. While cnidarians (the phylum to which corals belong) are known to lack an adaptive immune system, they demonstrate a precise ability to select for certain symbionts while generally keeping healthy and pathogen-free. This research pursues the proteins and interactions involved in cnidarian immunity.

Corals are difficult to keep and grow in a laboratory setting, so instead, *Aiptasia pallida*, a sea anemone and cousin of coral, is used as a model organism. To determine protein interactions in *A. pallida*, I used a yeast two-hybrid screen. Ten *A. pallida* genes, found to have homology to scavenger receptors and TIRs (innate immune proteins in other animals), were identified and selected for the screen. These genes are called the "bait", and we are finding interactors with these genes using a library of "prey", which are all the other proteins in *A. pallida*. So far, these genes have been amplified and cloned into yeast and a couple of them appear to be producing protein. This screen is still ongoing, but will shed insight into the immune pathway of *A. pallida* and perhaps other cnidarians like corals.

Propranolol as an adjunct to exposure therapy in the treatment of pathological fear memory: an animal model

Wendy Tan, Danya Potter, Emma Close, Allen Schneider
Swarthmore College Department of Psychology
wtan1@swarthmore.edu

Clinical studies have shown that a therapeutic procedure known as exposure therapy – the gradual exposure to a feared object in the absence of actual harm – is effective in reducing abnormal fear memory. The treatment, however, is limited: the abnormal fear memory often returns.

In a recent experiment, we used an animal analogue of exposure therapy, referred to as extinction training, to limit or prevent retention of fear. Twenty-four hours after fear conditioning (in which a mild foot-shock was administered in a dimly lit compartment), animals received a brief 30 sec exposure to the apparatus in the absence of shock. That is, in contrast to the standard extinction procedure in which fear increases with increasing exposure, the animals were removed from the apparatus before the level of fear developed to a significant degree. A retention test administered the next day revealed that the brief exposure procedure was indeed effective in reducing retention of fear.

The present experiment determined whether the effectiveness of the brief exposure procedure (and by inference, exposure therapy in clinically traumatized patients) in reducing retention of fear could be augmented by co-administration of the antianxiety drug propranolol.

The experimental procedure consisted of three stages: fear conditioning (on day 1), 30 sec exposure to the apparatus in the absence of shock (on day 2) and a retention test (on day 3). Propranolol or saline was administered 20 min prior to the brief exposure, the time required for the drug to reach the brain. Retention of fear was assessed by returning the animals (drug-free) to the conditioning apparatus in the absence of shock and monitoring fear-related (freezing) behavior.

The results indicated that propranolol, relative to saline, had two effects: 1) it reduced retention of fear during the 30 sec exposure itself and 2) it reduced retention of fear 24 hours later, after the drug was cleared from the system. To account for the results, we propose that the 30 sec exposure serves as a learning experience during which the animals learn to associate weak fear with the apparatus – and propranolol, by further reducing fear, enhances conditioning of weak fear during the 30 sec exposure and enhances retention of weak fear in drug-free animals the next day.

Ongoing experiments in our laboratory are investigating the mechanism underlying propranolol's effectiveness in reducing fear, specifically its effect as both a protein synthesis inhibitor and a beta-adrenergic blocker on reconsolidation of newly retrieved fear memories.

With respect to the clinical implications, until a more complete dose-response drug study is conducted, it would be premature to draw conclusions regarding the effectiveness of propranolol as a potential adjunct to exposure therapy.

Failed Power Domination

Jonathan Tostado-Marquez, Cheryl Grood & Thomas Hunter

Swarthmore College, PA
jtostad1@swarthmore.edu

Abstract

A power dominating set of a graph G is a subset S of vertices of G for which application of the power domination process results in all vertices joining S. The first part of power domination process enlarges S by adding to it all of its neighbors: that is, if u is neighbor of a vertex in S, then u joins S. The next step of the process states that if there is a vertex v in S that has exactly one neighbor u not in S, then u joins S. This step is iterated until there are no more vertices in S with exactly one neighbor not in S. This process of adding certain vertices to an initial set of vertices S is modeled after the monitoring of electrical networks by phase measurement units (PMUs), where electric nodes correspond to vertices, edges represent transmission lines connecting the nodes, and PMUs are placed at the vertices initially in S.

We introduce a new graph parameter, the failed power domination number of a graph G, $F_P(G)$, to be the maximum cardinality of a subset S of vertices of G that is not a power dominating set. We determine formulas for the failed power domination number of several graph families, including complete graphs, multipartite graphs, and the Cartesian product of a cycle and P_2. We also determine a formula for the failed power domination number of the corona of two graphs.

Works Cited

Fetcie et al., The failed zero forcing number of a graph, Involve 8 (1) (2015) 99-117.

Ansill et al., Failed skew zero forcing on a graph, Linear Algebra and its Applications 509 (2016) 40-63.

Benson et al., Zero forcing and power domination for graph products, 2015.arXiv:1510.02421.

Investigating the effects of antioxidants SkQ1 on mtDNA in PolG mouse fibroblasts

Soumba Traore, Konstantin Khrapko and Dori Woods

Northeastern University
Straore1@swarthmore.edu

Mitochondrial deterioration has been shown to be caused by reactive oxidative species (ROS) as well as an accumulation of mitochondrial DNA (mtDNA) mutations. As a result of the deterioration, aging occurs. In this study we used an antioxidant SkQ1 to counteract the ROS and mtDNA mutations. We conducted a short term and long term study with the objective of observing the affect of SkQ1 on first generation mice with the proofreading deficient version of mtDNA polymerase gamma (PolG) . In our short-term study, we ran six treatments to determine the affect on SkQ1 on cells treated with oxidizing agents such as hydrogen peroxide and paraquat. In our long-term study, we passaged two distinct cell lines for nine weeks to determine the rate of mutation accumulation for cells treated with and without SkQ1. Since this is a replication study, our results from PCR analysis, cell imaging assays and DNA sequencing should indicate that SkQ1 reverses the effects of the pro-oxidants on fibroblasts cells and decreases the rate of mutation accumulation. Our result did not demonstrate that SkQ1 as an antioxidant is necessary for decreasing oxidative stress, rather they suggest that SkQ1 suppresses cell proliferation. Future studies will include more analyses of short and long-term assays to further understand the role of SkQ1 in effecting mitochondrial diseases with similar mitochondrial damages to PolG mice mitochondrial damage.

Exploration of Asymmetrical Gene Expression within *Ciona Intestinalis*

Cameron Tumey, Brad Davidson
Swarthmore College
ctumey1@swarthmore.edu

The processes underlying left- right asymmetry are highly conserved across a wide range of species. Nodal signaling, H+/K+ ATPase dependent ion flux and ciliary flow are required for lateral asymmetry in both protostome and deuterostome clades yet details regarding how these initial processes lateralize organ morphogenesis remain poorly characterized. We use the invertebrate chordate *Ciona intestinalis* to investigate asymmetric organ development along the left-right axis. In *Ciona,* the heart and endoderm are positioned to the right and this asymmetry arises simultaneously. Surprisingly, previous research indicates that *Ciona* heart asymmetry is dependent on ion flux but does not require Nodal signaling. To understand the link between ion flux and lateralized organ morphogenesis, we have begun to characterize laterally asymmetric gene expression in *Ciona* embryos. By sequencing RNA in thin sections spanning the left-right axis, we have established a list of 19 candidate genes displaying strongly lateralized expression including orthologs to *Cspp1, Gpr161, Taf9, Nup155, Lars2, FoxC, Siah1B*, and *Prmt9* that are strongly expressed on the right side of the embryo and *Tor1B, Sept9, Klhl4, Mef2, Pitx, Nodal, sFzd(Crd), Dnah8, Crkl, Lrrc46,* and *Kat2a* that are strongly expressed on the left side. We have confirmed six of these predicted expression patterns through in-situ hybridization. These studies have revealed that many of the candidate genes are expressed in the trunk lateral cell lineage, a group of mesodermal cells that migrate extensively in the larval head and differentiate into blood and muscle. We have also begun to characterize the dependence of these candidate genes on ion flux using the H+/K+ ATPase inhibitor omeprazole. The further characterization of asymmetrically expressed genes should provide critical insights into the molecular mechanisms driving heart and endoderm asymmetry within *Ciona* and vertebrate embryos.

Validating PTCHD1 removal from knockout mice lines that utilize Cre- lox recombinase system

Anthony Velleca

Brad Davidson

Feng lab, McGovern Institute for Brain Research at MIT and the Broad Institute

avellec1@swarthmore.edu

Hyper-aggression is a symptom of many autism spectrum disorder (ASD) patients (Pivovarciova et. al, 2014). Aggressive behavior is not unique to humans and is a common behavior in mice, meaning mouse models offer us an opportunity to study this innate social behavior and identify the neural circuitry regulating it. Previous work has identified several regions within the thalamus and hypothalamus that have been associated with aggression, including the medial and ventromedial hypothalamus (Wong et. al., 2016, Lee et. al., 2014).

One protein that the Feng lab focuses on is PTCHD1, which has been implicated in ASD and aggression. About 1% of patients with ASD and intellectual disability (ID) have a mutation in the PTCHD1 gene (Noor et. al., 2010). Humans with a PTCHD1 deletion display symptoms of ASD (Chaudhry et. al., 2015). Previous work from my summer lab demonstrated that when PTCHD1 is globally knocked-out in mice, the rodents display attention deficits, hyperactivity, learning impairment, motor defects, as well as hyper-aggression (Wells et. al., 2016). Thus, studying the gene PTCHD1 offers a viable window into the circuitry controlling aggression.

This past summer I contributed to this project by evaluating two particular lines of *Cre* mice: Vglut2-Cre, and VGAT-Cre. The Cre lines were generated so that the specific structures in the thalamus and hypothalamus are targeted. These mouse lines have been used for behavior testing and one line displayed an interesting phenotype. However, it was important to understand how well these Cre lines targeted PTCHD1positive (PTCHD1+) cells. My work focused on quantifying the overlap between the PTCHD1+ cells and the Cre+ cells to understand the percentage of cells rendered non-functional on a structure-by-structure basis. I sectioned, immunostained, and imaged brains from mice of these three lines and determined regions of Cre and PTCHD1 co-localization using reporter tags. Ultimately, I concluded that two of these cre lines are not reaching the majority of PtchD1 cells, which is critical for researchers on this project to know.

Zero-Diagonal Minimum Rank over Generalized Fields

Zara Williams-Nicholas, Cheryl Grood, and **Thomas Hunter**

Swarthmore College
zwillia1@swarthmore.edu

Abstract

The goal of the *minimum rank problem* is to determine the minimum rank of a given family of matrices associated with a particular graph. The classic minimum rank problem examines real, symmetric matrices whose diagonal is allowed to be free, and whose off-diagonal nonzero entries are determined by the edges of the graph. This problem has been studied extensively, along with its generalizations to other fields. In 2012, the minimum rank problem was investigated for real, symmetric matrices where the diagonal entries are restricted to be zero. We consider the minimum zero-diagonal rank problem over fields other than **R**.

Given a graph G with vertices $v_1, \ldots, v_n$ and a field $\boldsymbol{F}$, we say a symmetric matrix A in $M_n(\boldsymbol{F})$ is *associated with* G if the (ij)-entry of A is nonzero if and only if v_i is adjacent to v_j. Let $S^{\boldsymbol{F}}(G)$ denote the set of all matrices in $M_n(\boldsymbol{F})$ associated with G and define $mr_0^{\boldsymbol{F}}(G) = \min \{A \mid A \text{ is in } S^{\boldsymbol{F}}(G)\}$. For certain graph families, including cycle graphs and tadpole graphs, we are able to determine $mr_0^{\boldsymbol{F}}(G)$ for all fields $\boldsymbol{F}$. We also extend work of Leong (2014) to compute $mr_0^{Z2}(G)$ for additional graph families.

Literature Cited

C. Grood and T. Hunter. Realizable ranks with zero diagonal, *preprint*.

C. Grood, J. Harmse, L. Hogben, T. Hunter, B. Jacob, A. Klimas, S. McCathern. Minimum rank with zero diagonal. *Electronic Journal of Linear Algebra*, 27:458 - 477, 2014.

C. Grood, T. Hunter, O. Leong. Ranks of graphs over $\mathbf{Z}_2$, *preprint*.

C. Cain. Minimum ranks of graphs with six vertices and general conjectures, *preprint*.

Aluminum Complexes of Redox Active Ligands

Henry Wilson, Christopher R. Graves

Swarthmore College
Hwilson1@swarthmore.edu

In the field of chemistry, there has been a widespread shift towards developing greener chemical processes to diminish the environmental cost of chemical reactions. One such set of reactions is known as redox reactions, which involve the transference of electrons between compounds. Typically, these electron transfers require the aid of a transition metal catalyst such as palladium or platinum to proceed. The cost of these transition metals can exceed $30,000 per kilogram, and the metals can be environmentally costly to acquire. Aluminum presents an appealing alternative, making up roughly 8% of earth's crust and costing a mere $2 per kg. Aluminum itself, however, is not particularly redox active, and its various redox states are difficult to access. This project focused on the design of ligands with multiple accessible redox states when complexed to an aluminum center in order to grant aluminum redox catalysis capability. The ligand design is centered around an α-diimine structure whose multiple redox states are stabilized by a para substituted aromatic substituent and the aluminum center. The aromatic substituent was varied based on electron donating/withdrawing properties, so that the effect of electron density in the diimine could be observed. Compounds containing various substituents on the aromatic ring were synthesized, characterized, and their electrochemical properties recorded. This research will be valuable in the development of aluminum as a catalyst to replace current transition metal catalysts in use.

Aluminum Complexes of Nitroxide-Based Redox-Active Ligands

Audra Woodside, Mackinsey Smith, Christopher Graves

Swarthmore College, Department of Chemistry
awoodsi1@swarthmore.edu
msmith7@swarthmore.edu

The development of aluminum complexes implementing redox-active ligands has the potential to significantly broaden the reaction chemistry of the element through expansion into redox-based chemistries. We report the synthesis of aluminum coordination complexes implementing redox-active nitroxide based ligands. Specifically, we present our work on the $N(benylNO)_3Al$ system where the nitroxide ligand complex extends multi-electron redox chemistry to the complex. Characterization including ^1H NMR spectroscopy, X-ray diffraction, and cyclic voltammetry data will be presented in addition to our preliminary reactivity studies.

Learning Deviation Payoffs in Large Symmetric Games

Fengjun Yang, Professor Bryce Wiedenbeck

Swarthmore College, PA
fyang1@swarthmore.edu

Game theory, as a mathematical framework for analyzing multi-agent decision-making, has wide applications in social sciences. Exact analyses of large games, however, are computationally intractable, as the size of games stored in normal form grows exponentially to the number of players in a game. By sampling profile-payoff pairs and running regression over these sampled data, machine learning offers a way to convert normal-form games into a more compact functional representation. We show both theoretically and experimentally that this conversion has the potential to approximate exact analyses with less resources. Our algorithm samples a small proportion of complete profiles evenly over the profile space, with the only exception of oversampling on the edges. We then apply Gaussian process regression to approximate utility functions. These learned utility functions are used as the basis for approximate analyses of large games. We also propose a way to efficiently compute expected payoffs efficiently specifically when RBF kernel is used for the Gaussian process regression. This technique approximates the equation for exact computation by approximating multinomial distribution with a normal distribution and using integration to replace summation. Finally, we demonstrate experimentally that this algorithm shows strong potential by comparing the accuracy of payoffs estimated by learning with those estimated by Deviation Preserving Reduction, the state-of-the-art player-reduction method.

Simulating fibrin clot mechanics using finite element methods

Brandon Chung Yuen Yeung, E. Carr Everbach

Swarthmore College
cyeung2@swarthmore.edu

Blood clots inside blood vessels impede blood flow and can lead to blockage. Injection of thrombolytic agents affects the body systemically and may lead to haemorrhage. Risk is reduced with sonothrombolysis—high-amplitude pulsed ultrasound that drives micron-sized bubbles into violent oscillations, destroying the fibrin mesh of a clot. To gain insight into the 3D structure and mechanical behaviour of fibrin clots, we fabricated a clot from purified fibrinogen, imaged it using a confocal microscope and 3D printed a plastic model of the image. Coordinates of fibrin connection points were entered into ANSYS, the clot finite-element-simulated for nodal displacements, and the effective stiffness of the clot calculated. Simulations suggested that the elastic moduli in the three orthogonal directions were E_x = 113.5 Pa, E_y = 109.1 Pa, and E_z = 16.17 Pa. The close agreement between E_x and E_y supported the assumption of isotropy in a fibrin clot. The deviation of E_z from E_x and E_y could be attributed to the presence of the glass coverslip affecting the clot structure, and to the smearing of confocal micrographs in the z-direction effected by the microscope. Overall, results showed that confocal microscopy and finite element simulations in ANSYS are useful techniques for performing mechanistic studies on fibrin clots. Our next step is to simulate microbubble activity inside the virtual clot.

Microplastic pollution and its effects on *Aiptasia pallida*

Gun Min (Chris) Youn and Miranda Amilcar, Elizabeth Vallen and Rachel Merz

Swarthmore College
gyoun1@swarthmore.edu, mamilca1@swarthmore.edu

Plastic pollution is a major ecological concern in today's environment. However, one aspect of plastic pollution that has been relatively overlooked is microplastics, which are plastic particles less than 5mm in size. Our research focuses on microfibers, a subcategory of microplastics, and the impact different sized plastic fibers may have on the rate of food retention in the species *Aiptasia pallida.* Both long and short fibers were cut, dyed with a fluorescent dye, coated in brine shrimp extract, and fed to the anemones. Half the *Aiptasia* were also fed freshly hatched brine shrimp along with the fibers. Data on egestion were collected in 30 minute intervals over the course of 24 hours. After allowing a 24 hour resting period, the experiment was repeated once more. Short fibers were held in for a greater period of time than long fibers, and short fibers + shrimp were held in for the greatest period of time compared to all the other assays (SF = 450 min, SFS = 609 min, LF = 315 min, LFS = 473 min). This is of major concern because the assay in which the animals were fed shrimp most mimic the natural environment. Furthermore, based on SEM images taken after microfiber exposure, the *Aiptasia* suffered internal damage as the fibers ripped through their gastrovascular cavity as well as their body wall.